JGR Oceans

RESEARCH ARTICLE
10.1029/2022JC018964

Radium Inputs Into the Arctic Ocean From Rivers: A Basin-Wide Estimate

Emma J. Bullock[1], Lauren Kipp[2], Willard Moore[3], Kristina Brown[4], Paul J. Mann[5], Jorien E. Vonk[6], Nikita Zimov[7], and Matthew A. Charette[8]

[1]MIT-WHOI Joint Program in Oceanography/Applied Ocean Science & Engineering, Cambridge and Woods Hole, MA, USA, [2]Department for Environmental Sciences, Rowan University, Glassboro, NJ, USA, [3]Earth, Ocean, and Environment College of Arts and Sciences, University of South Carolina, Columbia, SC, USA, [4]Department of Fisheries and Oceans, Institute of Ocean Sciences, Sidney, BC, Canada, [5]Department of Geography and Environmental Sciences, Northumbria University, Newcastle Upon Tyne, UK, [6]Faculty of Science, Earth, and Climate, Vrije Universiteit Amsterdam, Amsterdam, The Netherlands, [7]North-East Scientific Station, Pacific Institute for Geography, Far-East Branch, Russian Academy of Sciences, Cherskiy, Russia, [8]Department of Marine Chemistry and Geochemistry, Woods Hole Oceanographic Institution, Woods Hole, MA, USA

Abstract Radium isotopes have been used to trace nutrient, carbon, and trace metal fluxes inputs from ocean margins. However, these approaches require a full accounting of radium sources to the coastal ocean including rivers. Here, we aim to quantify river radium inputs into the Arctic Ocean for the first time for ^{226}Ra and to refine the estimates for ^{228}Ra. Using new and existing data, we find that the estimated combined (dissolved plus desorbed) annual ^{226}Ra and ^{228}Ra fluxes to the Arctic Ocean are [7.0–9.4] × 10^{14} dpm y^{-1} and [15–18] × 10^{14} dpm y^{-1}, respectively. Of these totals, 44% and 60% of the river ^{226}Ra and ^{228}Ra, respectively are from suspended sediment desorption, which were estimated from laboratory incubation experiments. Using Ra isotope data from 20 major rivers around the world, we derived global annual ^{226}Ra and ^{228}Ra fluxes of [7.4–17] × 10^{15} and [15–27] × 10^{15} dpm y^{-1}, respectively. As climate change spurs rapid Arctic warming, hydrological cycles are intensifying and coastal ice cover and permafrost are diminishing. These river radium inputs to the Arctic Ocean will serve as a valuable baseline as we attempt to understand the changes that warming temperatures are having on fluxes of biogeochemically important elements to the Arctic coastal zone.

Plain Language Summary Radium (Ra) isotopes can be dissolved in water that comes into contact with minerals. Since they have varying half-lives, the ratio of Ra isotopes in water masses can help us understand where and how long ago Ra became dissolved in the water. As a result, these isotopes are powerful tracers of freshwater and shelf inputs into the ocean, which are important for nutrient, carbon, and trace metal fluxes. However, quantifying these inputs requires an understanding of all other radium sources to the coastal ocean, including rivers. The net ocean input of Ra isotopes from rivers must consider the freshwater dissolved load, as well as Ra desorbed from suspended particles in river estuaries. This study quantifies river radium inputs into the Arctic Ocean using dissolved concentrations and desorption experiments on riverine sediment. We find that Arctic rivers may have removal processes impacting Ra transport through estuaries that have not been observed in other regions. We also estimate the total riverine Ra inputs to the global ocean by adding data from 20 major rivers. These findings show that ~11% of all riverine Ra inputs to the global ocean come from Arctic rivers.

Key Points:

- This study quantified riverine ^{226}Ra and ^{228}Ra fluxes into the Arctic Ocean and provides the first Ra desorption data for Eurasian rivers
- North American rivers contribute the majority of riverine radium to the Arctic Ocean, due to higher desorption rates and sediment loads
- The Arctic Ocean receives an amount of riverine radium proportionate to its river water discharge: 11%–12% of the global riverine Ra flux

Supporting Information:

Supporting Information may be found in the online version of this article.

Correspondence to:

E. J. Bullock,
ebullock@whoi.edu

Citation:

Bullock, E. J., Kipp, L., Moore, W., Brown, K., Mann, P. J., Vonk, J. E., et al. (2022). Radium inputs into the Arctic Ocean from rivers: A basin-wide estimate. *Journal of Geophysical Research: Oceans*, *127*, e2022JC018964. https://doi.org/10.1029/2022JC018964

Received 28 JUN 2022
Accepted 25 AUG 2022

Author Contributions:

Conceptualization: Emma J. Bullock, Lauren Kipp, Matthew A. Charette
Data curation: Emma J. Bullock, Willard Moore, Kristina Brown, Jorien E. Vonk, Nikita Zimov, Matthew A. Charette
Formal analysis: Emma J. Bullock, Lauren Kipp, Willard Moore, Paul J. Mann, Matthew A. Charette
Funding acquisition: Matthew A. Charette
Investigation: Emma J. Bullock, Lauren Kipp, Kristina Brown, Jorien E. Vonk, Nikita Zimov, Matthew A. Charette

1. Introduction

Radium (Ra) isotopes have been used for decades to track sediment-water interactions, and provide a method to differentiate nutrient and trace metal inputs from shelves, rivers, and groundwater (e.g., Moore & Krest, 2004; Peterson et al., 2013; Tomasky-Holmes et al., 2013). While they themselves are soluble in seawater, ^{226}Ra and ^{228}Ra are supplied by the radioactive decay of their sediment-bound parent isotopes, ^{230}Th and ^{232}Th respectively (Moore & Edmond, 1984). With half lives of 5.8 years for ^{228}Ra and 1,600 years for ^{226}Ra, the distribution of these isotopes in the marine environment is controlled by different factors (Elsinger & Moore, 1980; Rutgers van der Loeff et al., 2003; Webster et al., 1995). The half life of ^{226}Ra is on the same order of magnitude as the global ocean overturning circulation, causing the distribution of ^{226}Ra in the ocean to be primarily controlled by slow removal from the surface ocean and release from marine sediments (Rutgers van der Loeff

Methodology: Emma J. Bullock, Lauren Kipp, Nikita Zimov, Matthew A. Charette
Project Administration: Matthew A. Charette
Resources: Kristina Brown, Paul J. Mann, Jorien E. Vonk, Nikita Zimov
Supervision: Matthew A. Charette
Validation: Matthew A. Charette
Writing – original draft: Emma J. Bullock
Writing – review & editing: Lauren Kipp, Willard Moore, Kristina Brown, Paul J. Mann, Jorien E. Vonk, Nikita Zimov, Matthew A. Charette

et al., 2003; Webster et al., 1995). With a considerably shorter half-life, the distribution of ^{228}Ra in the ocean is more restricted, the result being that ^{228}Ra has much higher relative activities close to the source of its release, such as over continental shelves, river mouths, or near submarine groundwater discharge (Moore et al., 1986; Moore & Shaw, 2008). As such, ^{228}Ra can be used to pinpoint solute sources from estuarine, fluvial, and shelf inputs to the open ocean (Moore et al., 1986; Moore & Krest, 2004; Moore & Todd, 1993; Rutgers van der Loeff et al., 1995).

Recent studies have found that the largest source of ^{228}Ra to the Arctic Ocean comes from continental shelves and that shelf inputs have increased substantially over the past decade (Kipp, Charette, et al., 2018; Kipp, Sanial, et al., 2018; Kipp et al., 2019; Kipp et al., 2020; Rutgers van der Loeff et al., 2018). However, rivers are also an important Ra source and it is currently unknown whether they are similarly sensitive to changing fluxes. Physical and biogeochemical processes in the Arctic Ocean are uniquely dependent on riverine inputs, due to the fact that despite having just 1% of the ocean's volume, the Arctic Ocean receives 10% of global river discharge (McClelland et al., 2012). Such a large influx of freshwater helps create a highly stratified surface layer in the Arctic Ocean, limiting upwelling and increasing the biogeochemical influence of riverine inputs on the upper water column (Kipp et al., 2020; Klunder et al., 2012). Along with Ra, rivers in the Arctic are known to contain high organic matter (OM) concentrations, accounting for 25% of the dissolved organic carbon supply to the central Arctic Ocean (Wheeler et al., 1997). They have also been shown to be a major source of trace metals to the Arctic Ocean, such as iron (Fe) and manganese (Mn) (Charette et al., 2020; Klunder et al., 2012; Middag et al., 2011).

Despite the potential for Ra to differentiate inputs from shelves, rivers, and groundwater, few studies have specifically investigated fluvial radium inputs to the Arctic Ocean. Radium can be both dissolved in rivers and released from suspended sediments in the estuarine mixing zone (Li et al., 1977; Rutgers van der Loeff et al., 2003). This desorption of Ra occurs along the salinity gradient as the fresh river water mixes with the ocean endmember, peaking at low to intermediate salinities (Elsinger & Moore, 1980; Li & Chan, 1979; Moore & Shaw, 2008; Webster et al., 1995). Rutgers van der Loeff et al. (2003) was one of the first studies to report dissolved radium measurements in major Arctic rivers (the Ob, Lena, and Yenisey rivers). Kipp et al. (2020) added North American river radium measurements (the Mackenzie and Yukon rivers). In another study, the authors used the weighted average of dissolved radium from three of these major rivers (Ob, Lena, and Mackenzie), as well as the experimentally determined Mackenzie River desorption values with the recorded sediment load to make a scaled-up estimation of total ^{228}Ra added to the Arctic Ocean due to fluvial inputs (Kipp, Charette, et al., 2018; Kipp, Sanial, et al., 2018). However, it's known that sediment loads and other indicators like dissolved and particulate organic carbon are considerably different in North American rivers as opposed to Eurasian rivers, largely due to their distinct drainage basin characteristics (Amon et al., 2012; Holmes et al., 2002, 2012). These differences could impact the desorption of Ra from suspended sediments and have not been investigated for Eurasian rivers.

Using a combination of new and historical data, this paper aims to refine ^{228}Ra riverine fluxes and present the first ^{226}Ra riverine flux estimate to the Arctic Ocean. These estimates will aid in the use of Ra isotopes as tracers of sediment-derived material fluxes into this high latitude basin. This paper also helps establish baseline values for riverine Ra fluxes in the Arctic. As the Arctic warms in response to climate change, freshwater fluxes from rivers have been increasing (Déry et al., 2016; Haine et al., 2015; Holmes et al., 2002; Rawlins et al., 2010), and are projected to increase over the next few decades (Andreson et al., 2020; Wang et al., 2021). Greater understanding of Ra transport is further necessary for understanding processes impacting Ra transport - such as increased permafrost thaw (Biskaborn et al., 2019; IPCC, 2021) and increased coastal erosion (Günther et al., 2013; Irrgang et al., 2022) - have also been documented. Finally, using data from major global rivers, we present a new global river Ra flux estimate which allows us to put our Arctic results into a broader context.

2. Materials and Methods

2.1. Dissolved Riverine Ra Concentrations

Radium samples were collected in the Ellice River in August and September 2017, the Kolyma River in June and September 2019, and the Buskin, Sustina, Matanuska, and Knik Rivers (hereafter referred to as Southern Alaska Rivers) in September 2019 (Figure 1). The Ellice River is located in Nunavut, Canada, on the mainland side of the Canadian Arctic Archipelago. The Kolyma River is a major river in Siberia, draining into the East Siberian

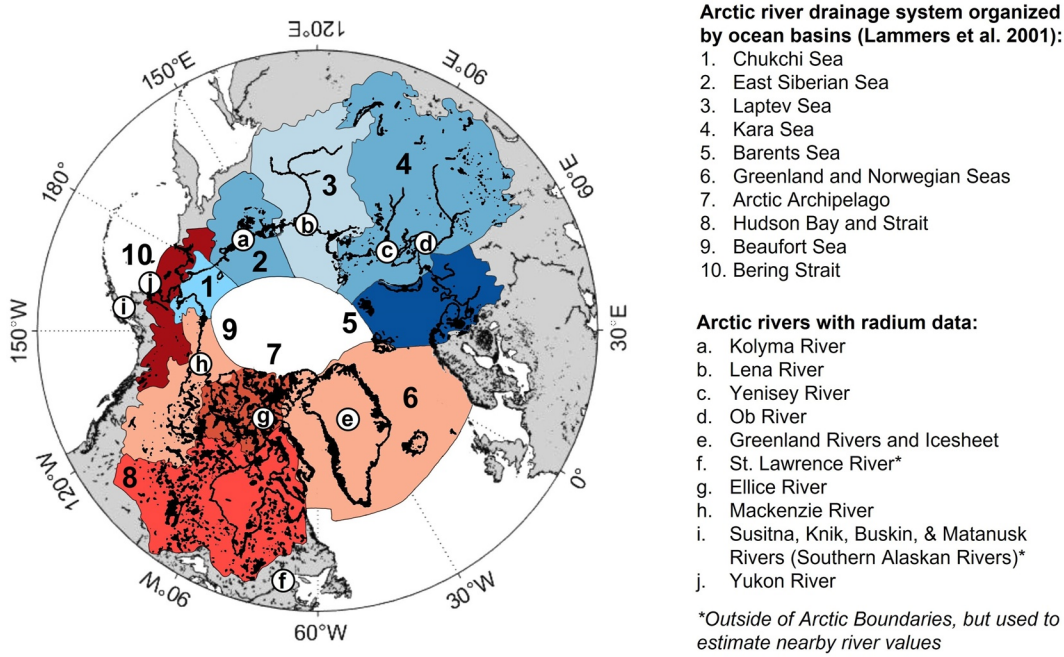

Figure 1. Map of Arctic with Arctic river drainage basins defined according to the methodology of Lammers et al. (2001) and labeled according to receiving marginal sea. North American drainage basins are represented in shades of red while Eurasian drainage basins are in blue. Arctic rivers with radium data are labeled at each river's mouth with white circles. Drainage basin and river names can be found in key.

Sea and represents the largest Arctic river basin underlain by continuous permafrost. The Buskin River is located on Kodiak Island, AK, while the Sustina, Matanuska, and Knik Rivers drain into Cook Inlet near Anchorage, AK. The samples were collected using either a bilge or well pump and the river water was passed through a 1 or 5 μm prefilter to remove suspended sediment before being filtered at <1 L/min onto Mn-coated acrylic fiber. The fiber was rinsed with Ra-free MilliQ water to remove any salts or sediment, then partially dried.

Samples with low activities (<0.4 dpm) were analyzed for ^{228}Ra via ^{228}Th ingrowth using a delayed coincidence counter (RaDeCC) (Moore, 2008), as described in Charette et al. (2015). Briefly, when ^{228}Ra is extracted onto the Mn fiber, ^{228}Th is extracted in parallel. Using the initial concentration of ^{228}Th and the concentration of ^{228}Th after 1–2 years, measured via RaDeCC, along with the decay constants of ^{228}Th and ^{228}Ra, the initial concentration of ^{228}Ra can be calculated. Low activity samples were analyzed for ^{226}Ra via ^{222}Rn emanation (Key et al., 1979), as described in Charette et al. (2015). Fibers were placed in a fiber holder that was then flushed with He for 5 min at 250 mL/min, sealed, and left for two weeks before analysis via ^{222}Rn ingrowth and scintillation counting. These two methods were used for low activity samples due to better method sensitivity than gamma counting (Charette et al., 2001), which was used for samples with high activities (>0.4 dpm per sample). For this method, the fibers were ashed (880°C, 16 hr), homogenized, capped with epoxy resin, and left for >3 weeks to obtain secular equilibrium between ^{226}Ra and its daughter radionuclides. The samples were then counted in a well-type gamma spectrometer for ^{228}Ra (via ^{228}Ac at 338 keV) and ^{226}Ra (via ^{214}Pb at 351.9 keV) (Charette et al., 2001).

2.2. Desorption Experiments

Suspended sediment from the Southern Alaskan Rivers was collected in September 2019 using a bilge pump to filter water through a 1 μm Hytrex filter. The filters were sealed in plastic bags and kept refrigerated until desorption experiments were performed. Bottom sediment from the Kolyma River was collected in summer 2018 from the Northeast Science Station in Cherskiy between July 23 to August 3. River bed sediment was sampled using a Van Veen grab-sampler and a stainless steel spoon, and stored in Whirl-Pak® bags. All samples represent recently deposited sediment rich in silt and clay in more quietly flowing locations of the river or delta. Within

12 hr after collection, sediments were frozen (−20°C) and remained so during transport. Sediment was thawed and dried before desorption experiments were performed in January and February 2022.

Desorption experiments were performed on suspended and recently deposited sediments from the Kolyma River and the Southern Alaskan Rivers. Two methods of desorption were performed based on the collection method of the suspended sediment. First, coastal seawater from Vineyard Sound was collected and filtered by the Environmental Systems Laboratory in Woods Hole, MA. The filtered seawater was then passed through manganese-oxide coated fibers (2 packed holders, 10 g each) at a flow rate of 0.5 L min^{-1} in order to remove Ra from the water. For each desorption experiment, 20 L of this filtered, Ra-free seawater was chilled to 4–6°C. For samples collected on cartridge filters, the filter was removed from its plastic bag and placed in an appropriately sized cartridge filter holder. A peristaltic pump circulated the filtered seawater through the filter at a rate of 1.25 L min^{-1} for 6 hr. This flow rate and length of time was chosen following preliminary experiments (S5.2) which showed that more radium was desorbed after 3 hours, but no significant increases in radium desorption occurred in exposures lasting longer than 6 hours. After 6 hr, the cartridge holders were removed and the seawater was filtered through Mn-coated acrylic fiber at a flow-rate ≤0.5 L min^{-1} for 3 hr. The fibers were treated and analyzed for radium isotopes using the same methods as the dissolved fibers (see above). The cartridge filters were ashed (500°C, 16 hr) in order to obtain the sediment weight for each sample.

The second method was performed on loose, recently deposited sediment from the Kolyma River, collected in 2018. Prior to the experiment, the sediment was packed into gamma counting vials and capped with a plastic vial cap. The sediment was then gamma counted using the same method as above, in order to get the bulk sediment ^{226}Ra and ^{228}Ra totals. The loose sediment (10–11 g) was then added to the seawater and was shaken every 15 min for 6 hr. The water was then filtered through two acrylic fiber filters to remove sediment, followed by a Mn-coated acrylic fiber (≤0.5 L min^{-1}) to collect Ra. The fibers were treated and analyzed for radium isotopes using the same methods as the dissolved fibers (see above). The percentages of Ra desorbed were then calculated by dividing the desorbed Ra values by the bulk Ra activities.

3. Results and Discussion

3.1. Radium in Arctic Rivers

3.1.1. Dissolved Radium Activities

Measured freshwater Ra concentrations in Arctic rivers (Table 1) range from 1.48 to 27.3 dpm/100 L (mean = 10.0 dpm/100 L) for ^{226}Ra and 2.52–40.9 dpm/100 L (mean = 16.9 dpm/100 L) for ^{228}Ra. Averages for the Eurasian continent were 11.7 dpm/100 L for ^{226}Ra and 19.3 dpm/100 L for ^{228}Ra. These are higher than North American averages: 8.70 dpm/100 L for ^{226}Ra and 11.7 dpm/100 L for ^{228}Ra (Table 1). The range of Arctic dissolved Ra values we report are comparable to dissolved concentrations found in rivers worldwide (Table S5). In non-Arctic rivers, freshwater dissolved ^{226}Ra values range from 2.74 to 24.5 dpm/100 L (global ^{226}Ra mean = 7.6 dpm/100 L; including Arctic = 7.9 dpm/100 L) and ^{228}Ra values range from 3.80 to 92.6 dpm/100 L (global ^{228}Ra mean = 16.4 dpm/100 L; including Arctic = 16.3 dpm/100 L). Our Arctic averages are slightly higher than global average concentrations (Figure 2), however we cannot discount the potential that this is due to insufficient sampling of Arctic freshwaters over the entire annual cycle. Arctic river discharge during the long winter season is typically low, followed by significant high discharge events during spring and moderate runoff over summer. The spring freshet event accounts for ∼50% of total annual discharge for the Kolyma and Yenisey rivers, and ∼30% for the Ob and Mackenzie rivers (Holmes et al., 2012). Significant seasonal changes in radium concentrations can occur over the hydrologic year as evidenced by measurements in the Mackenzie and Yukon rivers by Kipp et al. (2020). The majority of Ra measurements from Arctic rivers have been conducted during mid- to late-summer due to access and logistics, preventing us from using a weighted average based on seasonal river flow changes, which could impact our flux estimates.

3.1.2. Desorbed Radium From Suspended Sediments

To the best of our knowledge, this study presents the first radium desorption data for a Eurasian river. The total Ra present on the Kolyma sediments collected by this study were 1.6 ± 0.1 dpm/g for ^{226}Ra and 2.1 ± 0.5 dpm/g for ^{228}Ra. The amount desorbed was 0.33 ± 0.01 dpm/g for ^{226}Ra and 0.39 ± 0.05 dpm/g for ^{228}Ra. This results in a desorbable fraction of approximately 21% for ^{226}Ra and 19% for ^{228}Ra. The Mackenzie River has higher

Table 1
Measured Dissolved Ra Concentrations and Ra Desorption From Suspended Sediment in Arctic Rivers

River	Dissolved (dpm/100 L)		Desorbed (dpm/g)		Source
	^{226}Ra	^{228}Ra	^{226}Ra	^{228}Ra	
Yenisey (S)	3.25 ± 0.37	9.00 ± 1.34			Rutgers van der Loeff et al., 2003
Yenisey (W)	6.1 ± 0.7[a]	13.7 ± 2.1[a]			
Lena (S)	7.02 ± 0.37[b]	16.32 ± 2.34[b]			Rutgers van der Loeff et al., 2003; Charkin et al., 2020
Lena (W)	13.1 ± 0.4	24.9 ± 0.9			
Ob (S)	2.48 ± 0.37[b]	4.66 ± 1.25[b]			Rutgers van der Loeff et al., 2003
Ob (W)	27.3 ± 0.61	40.9 ± 3.7			
Mackenzie	17.37 ± 0.28	17.03 ± 1.02	0.47 ± 0.06[c]	0.94 ± 0.25[c]	Kipp et al., 2020
Yukon	14.35 ± 0.42	19.51 ± 1.81			Kipp et al., 2020; This Study
Kolyma	3.08 ± 0.41	2.52 ± 0.89	0.26 ± 0.02[c]	0.34 ± 0.07[c]	This Study
Ellice	1.48 ± 0.30	7.70 ± 1.54			This Study
St. Lawrence	2.55 ± 0.26	5.11 ± 0.51	0.32 ± 0.03	0.98 ± 0.10	Sérodes & Roy, 1983
Southern Alaska Rivers (Avg)	2.94 ± 0.42	3.88 ± 1.65	0.12 ± 0.05[c]	0.08 ± 0.02c	This Study
Greenland River and Ice Sheet	2.00 ± 0.02	23.00 ± 1.20	0.10 ± 0.03	0.42 ± 0.08	Linhoff et al., 2020

Note. Percent accounted for refers to how much annual discharge is accounted for based on our directly sampled rivers. (S) = Spring/Summer; (W) = Fall/Winter.
[a]Estimated based on % flocculated in Lena river, which contains similar DOC values. [b]Effective riverine endmember (by this studies' authors) based on salinity gradient through estuary after initial flocculation. [c]Experimentally determined through laboratory desorption experiments.

desorption rates for both isotopes: 0.46 ± 0.06 dpm/g for ^{226}Ra (14% desorbed) and 0.94 ± 0.25 dpm/g for ^{228}Ra (30% desorbed) (Kipp, Charette, et al., 2018; Kipp, Sanial, et al., 2018; Kipp et al., 2020). The Southern Alaskan Rivers had the lowest desorption rates: 0.12 ± 0.05 dpm/g for ^{226}Ra (14% desorbed) and 0.08 ± 0.02 dpm/g for ^{228}Ra (10% desorbed). Sediment grain size and mineralogy are key factors controlling differences in radium desorption behavior between rivers. Given the contrasting characteristics of Eurasian and North American river basins, it is unsurprising that the Kolyma desorption values are notably different from those reported for the Mackenzie River. Eurasian rivers, such as the Kolyma, drain large areas of low-relief tundra and wetlands, resulting in low suspended particulate loads but high dissolved organic carbon concentrations (Amon et al., 2012). Rivers in North America, by contrast, often drain mountainous regions and forests, where bedrock composition differs and high erosion rates result in considerable inorganic material fluxes to the Arctic Ocean (Amon et al., 2012). These high inorganic fluxes support higher desorption rates for North America compared to Eurasia. However, more data is needed to determine if the contrasting desorption rates are representative of their respective continents.

3.1.3. Flocculation in Eurasian Rivers

Numerous studies in temperate river estuaries have shown non-conservative addition at low- to mid-salinities (e.g., Li & Chan, 1979; Key et al., 1985). Values within the salinity mixing zone of the estuary that fall above the conservative mixing line have been attributed to radium desorption from suspended sediment (Elsinger & Moore, 1984; Krest et al., 1999). More recently, it has been learned that some of this non-conservative addition could be due to groundwater inputs or sediment resuspension (Moore & Shaw, 2008). However, Ra desorption from suspended sediments is still considered to be the major contributor of river-derived Ra to the coastal ocean (Cho et al., 2018; Kwon et al., 2014; Le Gland et al., 2017); this includes the Mackenzie River estuary (Kipp et al., 2020; Figure 3a).

However, a study of the Ob and Lena Rivers showed the opposite trend: a 50% and over 90% decrease in the freshwater Ra isotope activities at low salinities in the Lena and Ob Rivers, respectively (Rutgers van der Loeff et al., 2003). No apparent addition or removal of Ra isotopes was observed within the estuaries following this

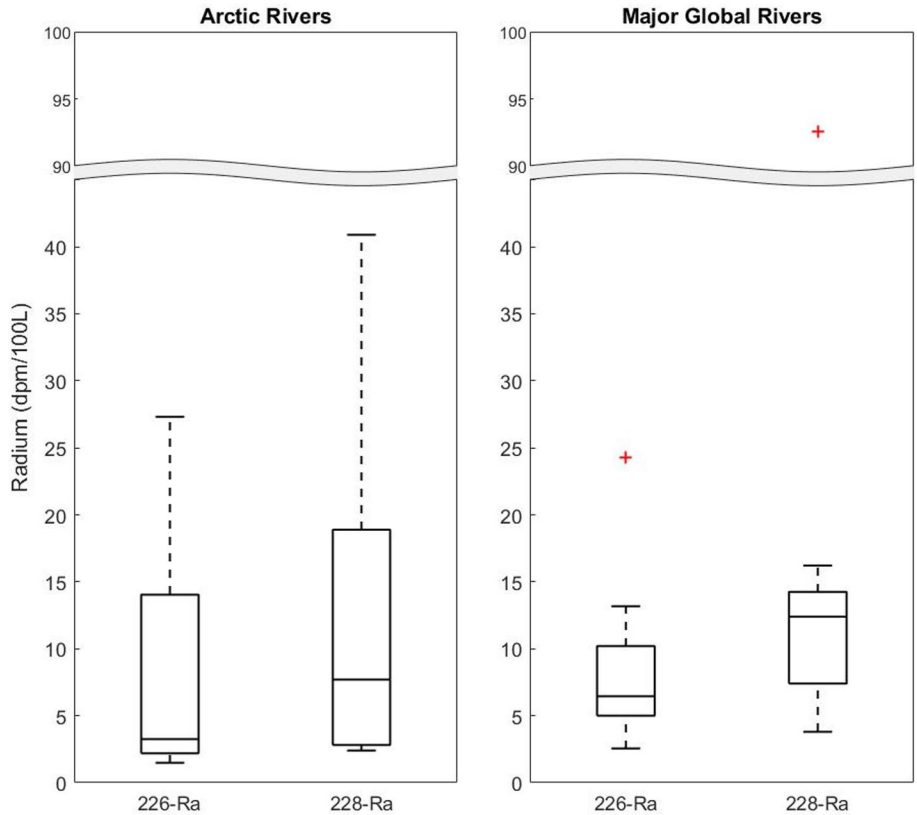

Figure 2. Box and whisker plot for Ra concentrations in fresh river water in Arctic rivers and major global rivers. It is important to note that the concentrations here reflect the actual freshwater concentrations, not the effective endmembers used in our input model for the Lena and Ob rivers. The outliers on the major global rivers plot are from the Parana and Uruguay river system.

initial decrease (Figure 3b). This study attributed the rapid removal of Ra in these estuaries to the high concentrations of dissolved organic carbon (DOC) present in these large Eurasian river systems, which have been shown to flocculate out of solution in the estuarine mixing zone (Rutgers van der Loeff et al., 2003).

Estuarine flocculation removal has also been reported for barium in the Ob and Yenisey Rivers (Ba; Guay & Falkner, 1998), which is known to behave similarly to Ra in riverine systems (Kipp et al., 2020; Moore & Edmond, 1984; Moore & Shaw, 2008). However, this process was observed only in samples collected during August, while samples collected in September showed no net removal. Due to the seasonality in removal, it was proposed that losses must be due to biological processes, or as a result of changing riverine organic matter composition between summer and fall (Guay & Falkner, 1998).

To gain a better understanding of this phenomenon, we examined two decades of seasonal measurements collected as part of the Arctic Great Rivers Observatory (Holmes et al., 2021; https://arcticgreatrivers.org/data/). We compared data for rivers previously reported to exhibit removal processes (Ob, Lena, & Yenisey) with those which have not (Kolyma, Yukon, & Mackenzie). We compared freshwater discharge, DOC, particulate organic carbon (POC), colored dissolved organic matter (CDOM), total suspended solids (TSS), particulate organic nitrogen (PON), nitrate (NO_3^-), ammonium (NH_4^+), temperature, alkalinity, and pH. Ice break up and thaw led to peaks in freshwater discharge, TSS, and DOC during June, with steady declines until winter baseline levels were reached in October or November across all rivers studied. Nutrients, such as organic nitrogen, followed opposing trends, likely due to uptake by microbes. DOC and CDOM concentrations were lower in our non-removal rivers (Kolyma, Yukon, and Mackenzie Rivers) relative to rivers where removal processes had been observed (Ob, Lena, and Yenisey), indicating that differences in organic matter concentrations and composition could be driving Ra removal processes in select Siberian rivers.

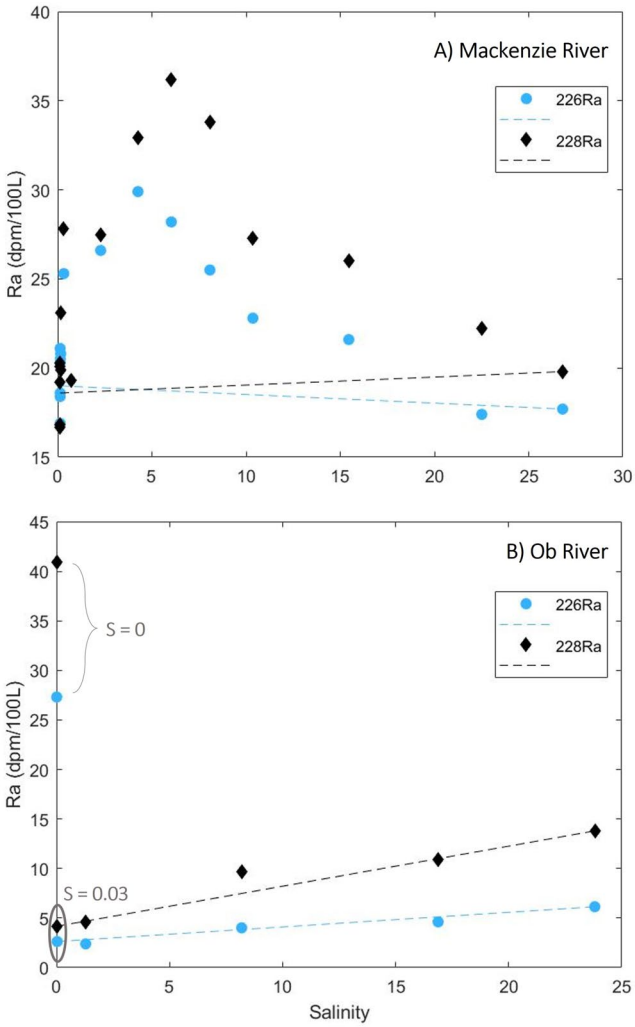

Figure 3. Ra concentrations and conservative mixing trends for two Arctic rivers. (a) values from the Mackenzie River estuary (North America), published by Kipp et al. (2020). Values above the conservative mixing line indicate inputs from groundwater or sediment desorption; (b) values from the Ob River estuary (Siberia), published by Rutgers van der Loeff et al. (2003). Intense flocculation removes most Ra from the Ob river at low salinities, requiring the use of a modified riverine end member that includes multiple processes (i.e., flocculation & desorption).

3.2. Calculations of Pan-Arctic Radium Flux Estimates

This paper uses the International Hydrographic Organization (IHO) definition of the Arctic (IHO, 2001), which also includes the Bering Strait and the Greenland and Norwegian Seas. River drainage basins are defined following the methodology of Lammers et al. (2001) and are referred to according to the receiving marginal sea (Figure 1). River discharge and sediment load values are shown in Figure 4 for gauged rivers (water discharge and sediment load estimates are provided in Supporting Information S1: Table S1).

Reported errors on Ra fluxes derived here represent those calculated for dissolved concentrations and desorption rates, and not for potential changes or variations in river discharge or sediment loads. Dissolved Ra concentrations have previously been determined for the Lena, Ob and Yenisey rivers on the Eurasian side of the Arctic, the Mackenzie, Yukon and St. Lawrence rivers on the North American side, and the Greenland ice sheet and rivers (Table 1). Here, we add dissolved data from the Kolyma River on the Eurasian continent, and data for the Ellice River and four Southern Alaska Rivers from North America. Radium desorbed from suspended sediment was calculated using suspended sediment loads and desorption values (dpm/g suspended sediment) based on the appropriate continent. The Mackenzie River desorption value was used for most of North America, with the following exceptions: the Bering Strait, where we used an average of the Mackenzie River's and Southern Alaska Rivers' desorption values, and Hudson Bay, which utilized estuarine data from the St. Lawrence River. The desorption value used for the Eurasian drainage basins was derived from our measurements from the Kolyma River.

In order to estimate total annual Ra fluxes from a river, the dissolved and desorbed inputs must be summed, as shown in Equation 1:

$$\mathbf{Ra_{Dis,\mathit{i}}} = \left(\boldsymbol{C_{fw,\mathit{i}}} \times \boldsymbol{D_{\mathit{i}}}\right) + \left(\boldsymbol{C_{d,\mathit{i}}} \times \boldsymbol{SS_{\mathit{i}}}\right) \quad (1)$$

$\mathrm{Ra}_{\mathrm{Dis},i}$ = total annual Ra inputs from river "i" (dpm y^{-1})

$C_{\mathrm{fw},i}$ = dissolved freshwater Ra concentration in river "i" (dpm m^{-3})

D_i = mean annual water discharge of river "i" (m^3 y^{-1})

$C_{d,i}$ = Ra desorption from sediments in river "i" (dpm g^{-1})

SS_i = mean annual sediment load of river "i" (g y^{-1})

To quantify the total river Ra flux to the Arctic Basin, we compared several scaling approaches. The most basic approach utilized average Ra data and total estimated water and sediment discharges for North America and Eurasia (Gordeev, 2006; Lammers et al., 2001), Greenland (Overeem et al., 2017), and Hudson Bay (Kuzyk et al., 2009). This approach took an average dissolved Ra concentration for all North American rivers with Ra data and multiplied it by the total North American river water discharge into the Arctic Ocean to estimate the dissolved flux. Similarly, it took the average North American sediment Ra desorption rate multiplied by the estimated sediment load from all North American Arctic rivers to derive the desorbed flux. Adding these terms together produced an averaged North American Arctic river Ra flux. This approach was repeated for Eurasia and Greenland, with the sum of the three results producing a pan-Arctic Ra river flux estimate that could account for broad differences between landmasses. This method was repeated using the median dissolved Ra concentrations and median sediment desorption rates, in case outliers were distorting the average.

While this approach is the most straightforward, it obscures any finer scale geographical differences that might be present. As a result, we used another approach that separated rivers based on their receiving marginal seas and scaled up by these drainage basins. For rivers with radium data and simple desorption behavior, Equation 1

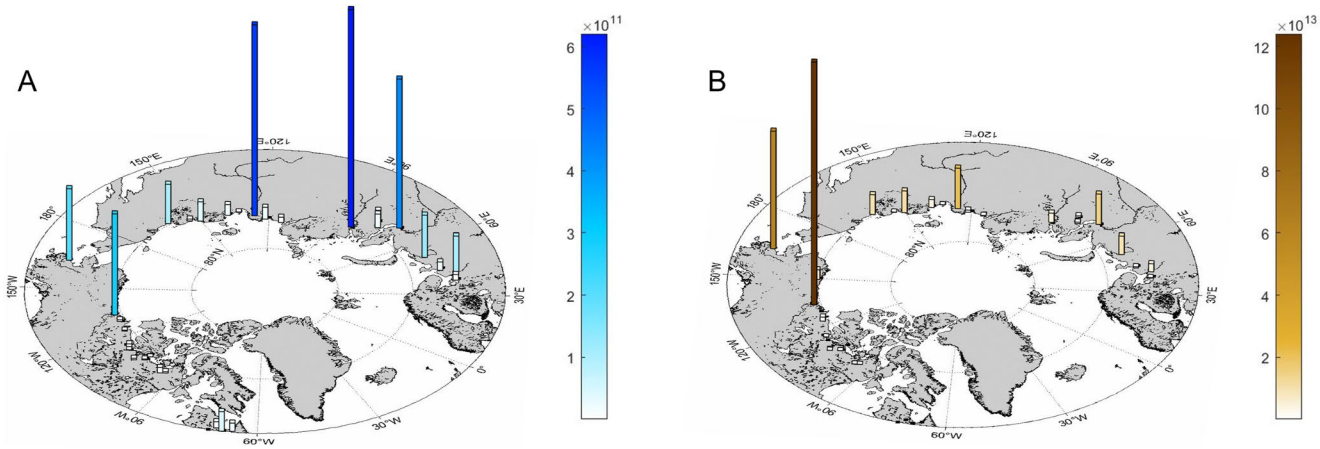

Figure 4. Maps of the Arctic showing (a) river water discharge ($m^3\ y^{-1}$) and (b) sediment load ($g\ y^{-1}$) for Arctic rivers with available river gauging and sediment load data (Refs: Table S1). Greenland water discharge is omitted from these figures as it also includes ice sheet contributions.

was used without modification. Monitored rivers without radium data were grouped based on proximity and watershed similarity to a major river that did have radium values (Table S2); for these groupings, Equation 1 was used with the assumption that the nearby major river Ra values were similar to those in the unsampled river. For all unaccounted for river discharge into each marginal sea, Equation 2 was used to scale up the Ra flux based on percent of water discharge remaining, following methods used in other flux studies (McClelland et al., 2016; Wheeler et al., 1997):

$$\mathbf{Ra_{MS}} = \sum_i \mathbf{Ra_{Dis,}}_i + \left[1 + \left(\frac{\boldsymbol{D}_{\mathbf{Basin}} - \sum_i \boldsymbol{D}_i}{\boldsymbol{D}_{\mathbf{Basin}}}\right)\right] \quad (2)$$

Ra_{MS} = estimated total annual Ra inputs to select marginal sea ($dpm\ y^{-1}$)

D_{Basin} = total estimated riverine flux for select river drainage basin ($m^3\ y^{-1}$)

For the Yenisey, Ob, and Lena Rivers, where flocculation has been observed during summer, different Ra values were employed for the fraction of water discharged in the summer versus the winter (Table 1). Based on the DOM data, we assumed that flocculation removal was restricted to June, July, and August. Using monthly discharge data between 2004 and 2020 (Holmes et al., 2021), we found that the average summer discharge accounts for 47% of the Yenisey River's annual discharge, 52% of the Ob's annual discharge, and 64% of the Lena's annual discharge. For this discharge we used the effective freshwater endmember Ra concentrations, after flocculation has led to some removal of Ra from the estuary, in order to calculate the summer Ra flux. For the remaining fall and winter discharge, we used Equation 1, with $C_{fw,\,i}$ equaling the pure freshwater/pre-removal Ra concentrations for the three rivers. The pre-removal concentration for the Yenisey River was estimated based on the percent removal that occurs in the Lena River, given its similar DOC and CDOM fluxes.

3.3. Total Riverine Radium Inputs to the Arctic Ocean

3.3.1. Total Riverine Flux of Radium to the Arctic Ocean

For the geographical separation method, the total dissolved flux is estimated at $(5.10 \pm 0.25) \times 10^{14}$ $dpm\ y^{-1}$ for ^{226}Ra and $(9.9 \pm 1.2) \times 10^{14}$ $dpm\ y^{-1}$ for ^{228}Ra (Table 2). The total desorbed flux from suspended sediments is estimated at $(3.96 \pm 1.50) \times 10^{14}$ $dpm\ y^{-1}$ for ^{226}Ra and $(6.58 \pm 2.87) \times 10^{14}$ $dpm\ y^{-1}$ for ^{228}Ra. The estimated total annual riverine ^{226}Ra and ^{228}Ra fluxes to the Arctic Ocean are $(9.06 \pm 1.37) \times 10^{14}$ $dpm\ y^{-1}$ and $(16.5 \pm 4.0) \times 10^{14}$ $dpm\ y^{-1}$, respectively. The total inputs calculated by using the averaging and median methods are slightly less than those found using the geographical separation method (Table 2), and all ^{228}Ra estimates fall slightly above the best estimate published by Kipp, Charette, et al. (2018); Kipp, Sanial, et al. (2018) but within their error: 12.6×10^{14} $dpm\ y^{-1}$ (range: 4.6–22.7 $\times 10^{14}$ $dpm\ y^{-1}$). Because of the good agreement between the methods, hereafter we will focus solely on the geographical separation method, since it allows us to better understand regional variations in Ra fluxes.

Table 2
Estimated Annual Riverine Ra Flux to Arctic Ocean by Ocean Basin

			Estimated Ra flux to Arctic Ocean (10^{12} dpm/y)					
Arctic Marginal Sea	Annual discharge (10^{11} m^3/y)	Percent accounted for	^{226}Ra	Error	Des. %	^{228}Ra	Error	Des. %
CAA	2.02	16%	4.06	0.94		17.7	3.9	
Barents Sea	4.46	60%	67.2	6.5		102	19	
Beaufort Sea	4.18	74%	156	46		239	120	
Bering Strait	3.12	72%	87.9	7.8		141	91	
Chukchi Sea[a]	1.20	0%	-	-		-	-	
East Siberian Sea	2.43	71%	15.3	1.6		16.4	18.9	
Hudson Bay	9.68	2%	28.9	5.0		80.5	23.4	
Kara Sea	12.3	91%	110	7		199	29	
Laptev Sea	7.63	82%	73.2	3.1		152	24	
Greenland	4.90		34.5	6.47		216	24	
N. America Total	19.6	30%	601	49	49%	946	285	44%
Eurasia Total	28.0	78%	271	14	29%	484	89	29%
Pan-Arctic Total	52.5	62%	906	137	44%	1650	400	60%
Averaging Pan-Arctic Total	52.5	NA	750	50	44%	1640	180	53%
Median Pan-Arctic Total	52.5	NA	820	280	51%	1240	450	45%

Note. Data and methods can be found in supplementary information. Des. = Desorption; CAA = Canadian Arctic Archipelago.
[a]Chukchi Sea had no rivers matching the criteria.

Despite Eurasian runoff delivering 1.4 times the freshwater to the Arctic Ocean as from North America, it contributed 2.2 times less ^{226}Ra and 2.0 times less ^{228}Ra per year (Table 2). This is driven by lower relative sediment loads and desorption rates as compared to the North American rivers. Eurasian rivers derive just 29% of their ^{226}Ra and ^{228}Ra fluxes from desorption, while this process accounts for roughly 49% and 44% of North American ^{226}Ra and ^{228}Ra inputs, respectively. These differences are likely due to a combination of higher organic to mineral ratios in suspended material in Eurasian rivers (Amon et al., 2012) and seasonal Ra removal within certain estuaries (Rutgers van der Loeff et al., 2003).

3.3.2. Arctic Riverine Fluxes Relative to Other Sources of Ra

Significant sources of Ra to the Arctic Ocean include advection through the Bering Strait and from the North Atlantic, diffusion from continental shelves, rivers, and ice-rafted sediment (Kadko & Muench, 2005; Kipp, Charette, et al., 2018; Kipp, Sanial, et al., 2018). Our ^{228}Ra river flux accounts for 5.5% of all ^{228}Ra inputs to the Arctic Ocean, with the largest input to the Arctic Ocean proper coming from continental shelves (92%; Kipp, Charette, et al., 2018; Kipp, Sanial, et al., 2018). Using the same methods as in Kipp, Charette, et al. (2018); Kipp, Sanial, et al. (2018) we estimate inputs for ^{226}Ra, with activities of ^{226}Ra isotopes that were measured on the 2015 U.S. GEOTRACES Arctic Transect (GN01) (for details, see Kipp, Charette, et al., 2018; Kipp, Sanial, et al., 2018). Briefly, Atlantic inflow was estimated to contain 6.3 Sv of water with a concentration of 7.43 dpm/100 L (Besqcqynska-Moller et al., 2012; Rudels et al., 2015), the Bering Strait was estimated to contribute 1.1 Sv with a concentration of 12.1 dpm/100 L (Woodgate et al., 2012), giving us advective inputs of 1.90×10^{16} dpm y^{-1}. Shelf inputs were estimated using a shelf area of 7.94×10^{12} m^2 (Jakobsson, 2002) and an activity of 1,070 dpm m^{-2} y^{-1}, for a total of 8.49×10^{15} dpm y^{-1}. Ice-rafted sediment activities were negligible. Consequently, rivers account for 3.2% of ^{226}Ra inputs to the Arctic Ocean proper, with shelves accounting for 29.8% and advection accounting for 67%.

Barium and Ba isotopes have previously been used to separate western versus eastern riverine inputs within the Arctic Ocean, while Ra isotope activity ratios (AR) have been used to track water masses within the Arctic Ocean (Kadko & Muench, 2005; Kipp, Charette, et al., 2018; Kipp, Sanial, et al., 2018; Kipp et al., 2019; Rutgers van der Loeff et al., 1995). North American rivers, including both dissolved and desorbed inputs, have a weighted ^{228}Ra/^{226}Ra AR of 1.56 while the Eurasian rivers have a weighted average of 1.84. These riverine

Table 3
Estimated Global Annual Riverine Ra Flux to Ocean

Ocean Basin	Annual discharge (10^{12} m^3/y)	Percent accounted for	Estimated Ra flux to Global Ocean (10^{14} dpm/y)					
			^{226}Ra	Error	Des. %	^{228}Ra	Error	Des. %
Atlantic	17.3	67%	27.3	16.2		49.6	12.6	
Pacific	8.25	18%	17.5	11.6		46.3	8.0	
Indian	3.80	54%	17.8	20.8		38.4	13.1	
Arctic	5.25	62%	9.06	1.37		16.5	4.0	
Baltic Sea	0.46	2%	0.15	0.04		0.21	0.03	
Combined: Black Sea, Red Sea, and Mediterranean	1.09	5%	1.36	0.16		1.67	0.34	
Global total	37.0	50%	73.2	50.2	79%	150	40	76%
Averaging global total	37.0	NA	170	130	83%	270	200	79%
Median global total	37.0	NA	150	20	85%	190	20	74%

Note. Des. = Desorption

ARs values are significantly lower than the AR ∼ 3.9 observed over the Laptev Shelf (Rutgers van der Loeff et al., 2003) and the AR ∼ 2.8 seen over the Chukchi shelf (Kipp et al., 2019; Vieira et al., 2019). This could allow differentiation between shelf and riverine Ra isotope inputs in certain regions of the Arctic Ocean, which has always been uncertain based on salinity alone (Kipp et al., 2019).

4. Arctic River Radium Fluxes in a Global Context

4.1. Total Riverine Flux of Radium to the Global Ocean

Ra data from 20 rivers were utilized, accounting for 50% of global riverine water discharge (Suzuki et al., 2018). Using the global median for riverine Ra concentrations and desorption rates (see Text S4), as well as global estimates for water discharge and sediment inputs (Overeem et al., 2017), the estimated global river ^{226}Ra and ^{228}Ra inputs are $(15 \pm 2) \times 10^{15}$ dpm y^{-1} and $(19 \pm 2) \times 10^{15}$ dpm y^{-1}, respectively, while the globally averaged estimate is somewhat higher: $(17 \pm 13) \times 10^{15}$ dpm y^{-1} and $(27 \pm 20) \times 10^{15}$ dpm y^{-1} for ^{226}Ra and ^{228}Ra, respectively (Table 3). Using an ocean basin approach, the annual ^{226}Ra and ^{228}Ra fluxes to the global ocean are $(7.4 \pm 5.0) \times 10^{15}$ dpm y^{-1} and $(15.3 \pm 3.8) \times 10^{15}$ dpm y^{-1}, respectively (Table 3; Text S4). For this approach, the Atlantic Ocean contributes the largest percentage of riverine radium inputs, followed by the Indian and Pacific Oceans. The Arctic Ocean receives 12% of global riverine ^{226}Ra inputs and 11% of ^{228}Ra inputs, similar percentages to global river discharge (McClelland et al., 2012). Considering the fact that the Arctic Ocean accounts for just 3% of the global ocean surface area, such high riverine Ra inputs result in rivers having a much larger impact on Arctic Ocean surface water Ra concentrations than would be observed in the Atlantic or Pacific Oceans.

The global estimates are in good agreement with literature estimates for ^{228}Ra (fluxes ranging from 12–37 $\times 10^{15}$ dpm y^{-1} (Cho et al., 2018; Kwon et al., 2014; Le Gland et al., 2017), and ^{226}Ra (estimate equaling $11.7 \pm 5.3 \times 10^{15}$ dpm y^{-1} (Xu et al., 2022)). The latter study utilized a Monte Carlo simulation with average ^{226}Ra concentrations from 13 rivers and average desorption values from 8 rivers to derive their riverine ^{226}Ra flux estimate. The discrepancy between our two approaches is much larger for the global estimates than it was for the Arctic estimates. The range in dissolved ^{226}Ra concentrations for the 30 rivers with available data was 1.48–24.3 dpm 100 L^{-1}. For ^{228}Ra the range is even larger: 2.4–92.6 dpm 100 L^{-1}. Thus, high outliers in these ranges drive up the global average and the median may not accurately capture this range. For the rest of our discussion, the globally averaged value is treated as an upper limit of potential riverine Ra inputs to the global ocean, while the ocean basin method is treated as a more realistic estimate.

4.2. Global Riverine Fluxes Relative to Other Sources of Ra

To place our global radium river fluxes in context, we compare it to other major sources of radium to the global ocean (Figure 5). Estimates for ^{228}Ra from SGD range from $(85 \pm 7) \times 10^{15}$ dpm y^{-1} (Le Gland et al., 2017) to

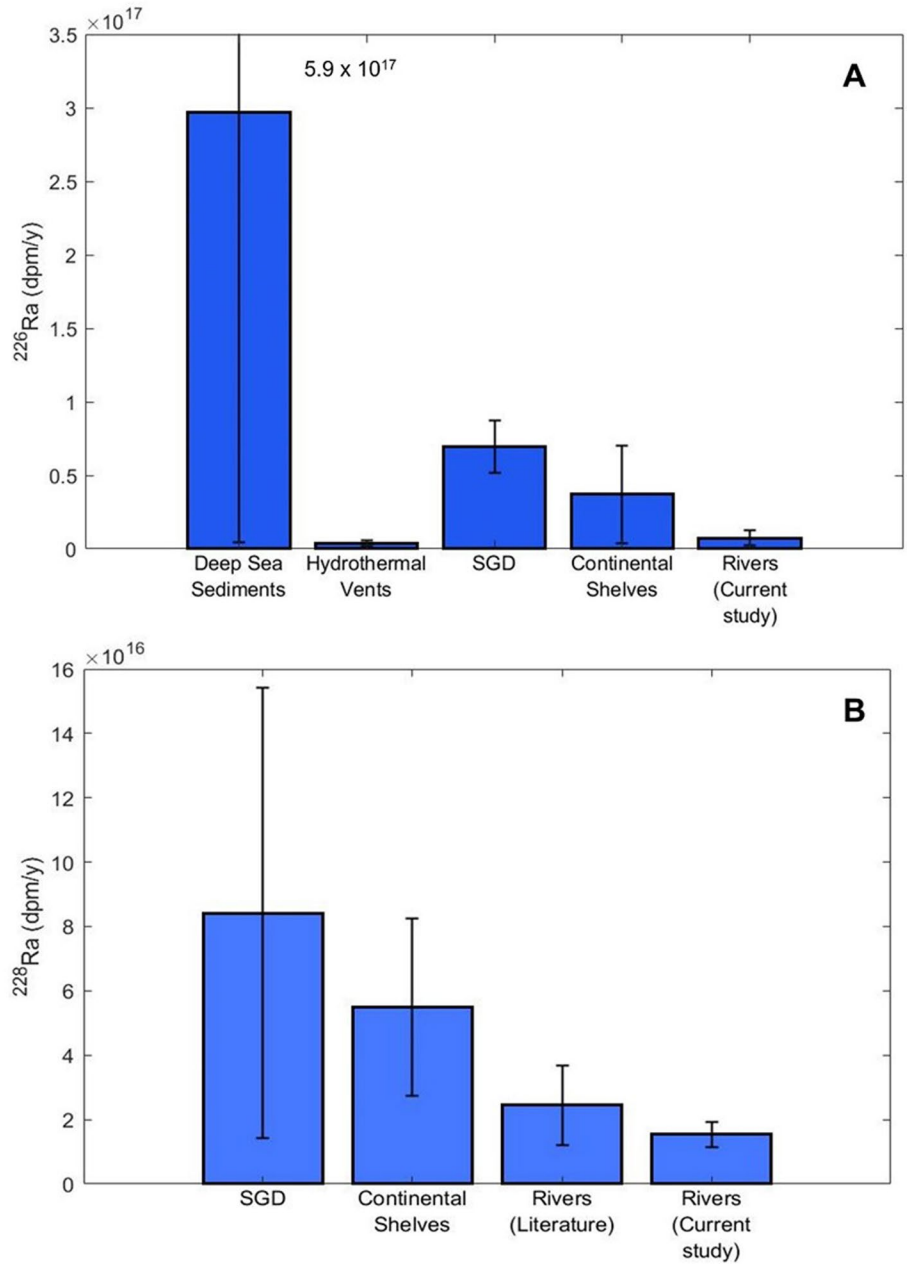

Figure 5. Boxplot of major Ra sources to the global ocean. (a) annual ^{226}Ra inputs to the global ocean (dpm/y). (b) annual ^{228}Ra inputs to the global ocean (dpm/y), omitting deep ocean inputs. SGD = Submarine Groundwater Discharge.

approximately 130×10^{15} dpm y^{-1} (Cho et al., 2018; Kwon et al., 2014). SGD inputs of ^{228}Ra are thus 5 to 9 times higher than the ^{228}Ra flux from rivers. For continental shelf sediments, Le Gland et al. (2017) estimated that ^{228}Ra fluxes fall between (9.9–150) $\times 10^{15}$ dpm y^{-1}, while Kwon et al. (2014) estimated this flux at 55×10^{15} dpm y^{-1}. Depending on the estimate, ^{228}Ra inputs from the shelves could either be on par with riverine inputs or up to 10 times greater. Dust can be neglected as it contributes <1% of ^{228}Ra inputs to the ocean (Kwon et al., 2014; Le Gland et al., 2017). A conservative estimate therefore places ^{228}Ra inputs from rivers around 10% of the total ^{228}Ra inputs to the global surface ocean.

Most studies have assumed that <10% of ^{226}Ra inputs to the ocean are sourced from rivers based on the flux required to close the ocean mass balance for ^{226}Ra (Ku & Luo, 1994, 2008). For SGD, Xu et al. (2022) reported a ^{226}Ra flux of $24 \pm 7 \times 10^{15}$ dpm y^{-1}. Our estimate, which used the global median groundwater ^{228}Ra/^{226}Ra

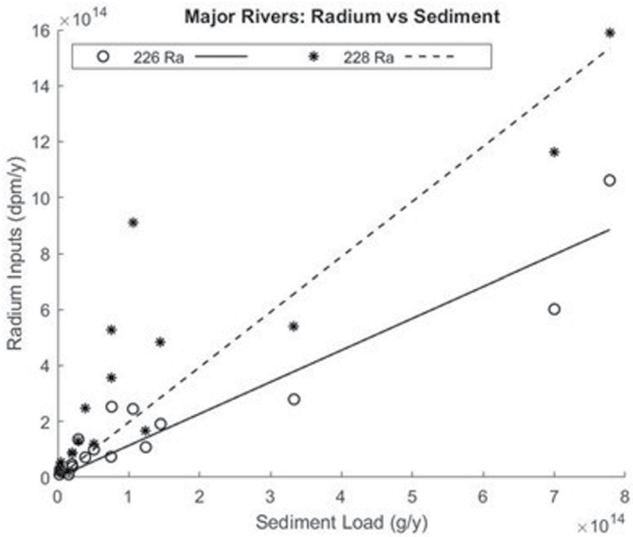

Figure 6. Total annual radium inputs compared to sediment load for major global rivers. The slopes are 1.1 ($R^2 = 0.88$) for ^{226}Ra and 2.0 ($R^2 = 0.74$) for ^{228}Ra.

AR (2.28; Charette & Moore, 2022) applied to the previously discussed model-derived ^{228}Ra SGD inputs, results in a flux range for ^{226}Ra from SGD of 37 × 10^{15}–57 × 10^{15} dpm y^{-1}. Using a continental shelf area of 2.73 × 10^{13} m^2, a ^{228}Ra flux from the shelves of (55 ± 50) × 10^{15} dpm y^{-1} (Kwon et al., 2014; Le Gland et al., 2017), and a continental shelf sediment AR of 1.5 (Moore & Shaw, 1998), we get a shelf ^{226}Ra flux of (37 ± 33) × 10^{15} dpm y^{-1}, in good agreement with the value of 42 × 10^{15} dpm y^{-1}, estimated by Xu et al. (2022). Deep sea sediment inputs have high errors, with diffusive fluxes ranging from 15 dpm m^{-2} y^{-1} to 2100 dpm m^{-2} y^{-1} (Costello et al., 2015). Using an intermediate diffusive flux estimate of 1,057 dpm m^{-2} y^{-1} and a deep sea sediment area of 2.81 × 10^{14} m^2 (Cochran & Krishnaswami, 1980) we get a ^{226}Ra deep sea sediment flux of ∼300 × 10^{15} dpm y^{-1}. Finally, hydrothermal vents are thought to supply ^{226}Ra to the ocean at a rate between 2–6 × 10^{15} dpm y^{-1} (Dymond et al., 1983; Kipp, Sanial, et al., 2018). Taken together, our estimate places ^{226}Ra inputs from rivers around 2% of the total ^{226}Ra inputs to the global ocean.

4.3. The Importance of Dissolved and Desorbed Inputs

Based on this study and other recent work, desorbed radium inputs dominate riverine radium fluxes to the global ocean (Kwon et al., 2014; Le Gland et al., 2017). This viewpoint was informed by early studies of radium desorption in rivers, where desorption was inferred from estuary mixing gradients (Elsinger & Moore, 1980; Li et al., 1977). It is now understood that submarine groundwater discharge can be a major source of radium to river estuaries (e.g., Krest et al., 1999; Luek & Beck, 2014). This process likely resulted in overestimates of the desorption Ra source during the formative years of radium studies in rivers. During these early studies, a proposed estimate of 2 dpm ^{228}Ra/g for desorbable radium became popular and has since been used in numerous studies and models to estimate desorption inputs to the ocean (Kwon et al., 2014; Le Gland et al., 2017; Moore et al., 2008).

To date, few studies have attempted to directly quantify Ra isotope desorption from riverine suspended sediment (Table 1; Table S5). However, with few exceptions, these desorption studies reported values below both the 2.0 dpm/g estimate and the theoretical approach by Webster et al. (1995). For the 20 rivers utilized in our global calculation, the range of desorbable ^{226}Ra is 0.21–2.74 dpm/g (mean = 1.08 dpm/g) and the range for ^{228}Ra is 0.39–5.97 dpm/g (mean = 1.63 dpm/g) (Table S5). For rivers where desorption experiments were not performed, the upper limit theoretical values from Webster et al. (1995) were used ($n = 3$) or the desorption rate was calculated based on estuarine inputs ($n = 5$). Both of these methods are likely to overestimate actual desorption contributions, highlighting the importance of performing desorption experiments, rather than relying on an average value from the literature, or on current theoretical models which do not take differences in mineralogy into account.

While rivers with large amounts of suspended sediment do tend to have inputs dominated by desorption, the story is more complex. Whether a river contributes more dissolved or desorbed radium depends on several factors, including the dissolved concentration, the desorbable radium per gram, and importantly, the suspended sediment concentration. Our data synthesis suggests that sediment load is more important to total riverine radium inputs than discharge (Figure 6). For example, despite the Congo River having 1.4 dpm/g more desorbable ^{226}Ra than the Amazon, the Amazon has a greater proportion of ^{226}Ra inputs from desorption because its suspended sediment load is 27 times higher. In contrast, smaller rivers tend to contribute proportionally higher amounts of dissolved radium. Rivers in this study had a range of relative dissolved inputs: 14%–99.9% with an average of 55% for ^{226}Ra and 11%–99.9% with an average of 56% for ^{228}Ra. As a result, it is most important to consider these factors when looking at individual river and coastal systems, since the overall weighted dissolved inputs to the global ocean remain low at 21% and 24% for ^{226}Ra and ^{228}Ra, respectively.

5. Conclusions

This study quantified riverine ^{226}Ra and ^{228}Ra fluxes into the Arctic Ocean and provides the first Ra desorption data for Eurasian rivers. It was found that North America contributes the majority of Ra from riverine fluxes to

the Arctic Ocean: 66% of ^{226}Ra and 57% of ^{228}Ra. This is due to larger suspended sediment inputs and higher desorption rates in North American rivers. Some Eurasian rivers' Ra inputs are also decreased due to organic matter flocculation in their estuaries, which can scavenge Ra before it reaches the coast. On a global scale, the Arctic Ocean collects a proportionate amount of Ra compared to its riverine inputs of 11%–12% the global total.

River and sediment inputs to the Arctic Ocean have increased over past decades due to warming temperatures and changing atmospheric moisture patterns, and are expected to increase in the future as warming continues (Andreson et al., 2020; Wang et al., 2021). Higher temperatures have also led to declining summer sea ice cover (Grosfeld et al., 2015; Serreze et al., 2006), more extensive permafrost thaw (Biskaborn et al., 2019; IPCC, 2021), and faster rates of coastal erosion (Günther et al., 2013; Irrgang et al., 2022). There is also evidence of increasing pore water exchange rates from continental shelves (Kipp, Charette, et al., 2018; Kipp, Sanial, et al., 2018; Rutgers van der Loeff et al., 2018), which may be linked to increased wave action and vertical mixing on shelves associated with the diminishing ice cover (Carmack & Chapman, 2003; Rainville & Woodgate, 2009; Williams & Carmack, 2015). Recently, groundwater has also been shown to be an important source of nutrients to the Arctic Ocean (Charkin et al., 2017; Connolly et al., 2020; Lecher, Chien, & Paytan, 2016; Lecher, Kessler, et al., 2016). This source is also predicted to increase with warming temperatures (Connolly et al., 2020; Nielson et al., 2018). All of these changes are expected to increase Ra inputs to the Arctic Ocean, which would impact the relative contributions of Ra sources, including that for rivers.

Although this study provides a baseline estimate for Ra contributions from rivers, future work is needed to capture changes in Ra fluxes as climate-driven changes occur in hydrology, groundwater supply and changing OM supply to coastal systems. Seasonal variability in Ra concentrations need to be further constrained, particularly during the high flow spring freshet. More work is also needed to determine whether desorption rates are consistent throughout continents, or whether rivers vary significantly. Finally, a better understanding is needed of the removal processes in Eurasian rivers. This is particularly important in terms of climate change, as warming temperatures and changing watershed conditions are shifting OM properties and distributions across coastal interfaces.

Data Availability Statement

Data from the Kolyma River, the Southern Alaskan Rivers, and previously unpublished submarine groundwater discharge data have been archived at the Biological and Chemical Oceanography Data Management Office (Biological and Chemical Oceanography Data Management Office (BCO-DMO). Dissolved radium data from these rivers can be found at https://www.bco-dmo.org/dataset/878527 [See citation below (Charette & Bullock, 2022b)]. Desorption data from these rivers can be found at https://www.bco-dmo.org/dataset/878663 (Charette & Bullock, 2022a). The submarine groundwater global database can be found at https://www.bco-dmo.org/dataset/878519 (Charette & Moore, 2022). These data are also available as supporting information.

Acknowledgments
The authors would like to thank Jessica Dabrowski, Juri Palmtag, Dirk Jong, Lisa Bröder, Kirsi Keskitalo, and the staff of the Northeast Science Station in Cherskiy for their assistance in sample collection in Alaska and Siberia. We would also like to thank Paul Henderson for his work in the field and for his help analyzing samples, and Heather H. Kim for her advice regarding statistical analyses. This study was a broad, collaborative effort that would not have been possible without contributions from numerous funding sources, including the National Science Foundation (NSF-0751525, NSF-1736277, NSF-1458305, NSF-1938873, NSF-2048067, NSF-2134865), the NERC-BMBF project CACOON [NE/R012806/1] (UKRI NERC) and BMBF-03F0806A, and an EU Starting Grant (THAWSOME-676982).

References

Amon, R. M. W., Rinehard, A. J., Duan, S., Louchouarn, P., Prokushkin, A., Guggenberger, G., et al. (2012). Dissolved organic matter sources in large Arctic rivers. *Geochimica et Cosmochimica Acta*, *94*, 217–237. https://doi.org/10.1016/j.gca.2012.07.015

Andreson, C. G., Lawrence, D. M., Wilson, C. J., McGuire, A. D., Koven, C., Schaefer, K., et al. (2020). Soil moisture and hydrology projections of the permafrost region - A model intercomparison. *The Cryosphere*, *14*(2), 445–459. https://doi.org/10.5194/tc-14-445-2020

Biskaborn, B. K., Smith, S. L., Noetzli, J., Matthes, H., Vieira, G., Streletskiy, D. A., et al. (2019). Permafrost is warming at a global scale. *Nature Communications*, *10*(1), 264. https://doi.org/10.1038/s41467-018-08240-4

Carmack, E., & Chapman, D. C. (2003). Wind-driven shelf/basin exchange on an Arctic shelf: The joint roles of ice cover extent and shelf-break bathymetry. *Geophysical Research Letters*, *30*(14). https://doi.org/10.1029/2003GL017526

Charette, M. A., Buesseler, K. O., & Andrews, J. E. (2001). Utility of radium isotopes for evaluating the input and transport of groundwater-derived nitrogen to a Cape Cod estuary. *Limnology and Oceanography*, *46*(2), 465–470. https://doi.org/10.4319/lo.2001.46.2.0465

Charette, M. A., & Bullock, E. J. (2022a). Desorbed radium from Kolyma (Russia), Ellice (Canada), and Kodiak Island (USA) rivers. Biological and Chemical Oceanography Data Management Office (BCO-DMO). (Version 1) Version Date 2022-08-16. https://doi.org/10.26008/1912/bco-dmo.878663.1

Charette, M. A., & Bullock, E. J. (2022b). Dissolved radium from Kolyma (Russia), Ellice (Canada), and Kodiak Island (USA) rivers. Biological and Chemical Oceanography Data Management Office (BCO-DMO). (Version 1) Version Date 2022-08-16. https://doi.org/10.26008/1912/bco-dmo.878527.1

Charette, M. A., Kipp, L. E., Jensen, L. T., Dabrowski, J. S., Whitmore, L. M., Fitzsimmons, J. N., et al. (2020). The Transpolar drift as a source of riverine and shelf-derived trace elements to the Central Arctic Ocean. *Journal of Geophysical Research: Oceans*, *125*(5), e2019JC015920. https://doi.org/10.1029/2019JC015920

Charette, M. A., & Moore, W. S. (2022). Measurements of global dissolved submarine groundwater discharge (SGD) 226-radium and 228-radium. Biological and Chemical Oceanography Data Management Office (BCO-DMO). (Version 1) Version Date 2022-08-16. https://doi.org/10.26008/1912/bco-dmo.878519.1

Charette, M. A., Morris, P. J., Henderson, P. B., & Moore, W. S. (2015). Radium isotope distributions during the US GEOTRACES North Atlantic cruises. *Marine Chemistry*, *177*(1), 184–195. https://doi.org/10.1016/j.marchem.2015.01.001

Charkin, A. N., Pipko, I. I., Pavlova, G. Y., Dudarev, O. V., Leusov, A. E., Barabanschikov, Y. A., et al. (2020). Hydrochemistry and isotopic signatures of subpermafrost groundwater discharge along the eastern slope of the Lena River Delta in the Laptev Sea. *Journal of Hydrology*, *590*, 125515. https://doi.org/10.1016/j.jhydrol.2020.125515

Charkin, A. N., Rutgers van der Loeff, M., Shakhova, N. E., Gustafsson, Ö., Dudarev, O. V., Cherepnev, M., et al. (2017). Discovery and characterization of submarine groundwater discharge in the Siberian Arctic seas: A case study in the Buor-Khaya Gulf, Laptev Sea. *The Cryosphere*, *11*(5), 2305–2327. https://doi.org/10.5194/tc-11-2305-2017

Cho, H.-M., Kim, G., Kwon, E. Y., Moosdorb, N., Garcia-Orellana, J., & Santos, I. R. (2018). Radium tracing nutrient inputs through submarine groundwater discharge in the global ocean. *Scientific Reports*, *8*(1), 2439. https://doi.org/10.1038/s41598-018-20806-2

Cochran, J. K., & Krishnaswami, S. (1980). Radium, thorium, uranium, and Pb-210 in deep-sea sediments and sediment pore waters from the North Equatorial Pacific. *American Journal of Science*, *280*(9), 849–889. https://doi.org/10.2475/ajs.280.9.849

Connolly, C., Cardenas, M. B., Burkart, G. A., Spencer, R. G. M., & McClelland, J. W. (2020). Groundwater as a major source of dissolved organic matter to Arctic coastal waters. *Nature Communications*, *11*(1), 1479. https://doi.org/10.1038/s41467-020-15250-8

Costello, M. J., Smith, M., & Fraczek, W. (2015). Correction to surface area and the seabed area, volume, depth, slope, and topographic variation for the World's Seas, Oceans, and Countries. *Environmental Science and Technology*, *49*(11), 7071–7072. https://doi.org/10.1021/acs.est.5b01942

Déry, S. J., Stadnyk, T. A., MacDonald, M. K., & Gauli-Sharma, B. (2016). Recent trends in variability in river discharge across northern Canada. *Hydrological Earth System Science*, *20*(12), 4801–4818. https://doi.org/10.5194/hess-20-4801-2016

Dymond, J., Cobler, R., Gordon, L., Biscaye, P., & Mathieu, G. (1983). 226Ra and 222Rn contents of Galapagos Rift hydrothermal waters - The importance of low-temperature interactions with crustal rocks. *Earth and Planetary Science Letters*, *64*(3), 417–429. https://doi.org/10.1016/0012-821x(83)90102-4

Elsinger, R. J., & Moore, W. S. (1980). 226Ra behaviour in the Pee Dee River-Winyah Bay estuary. *Earth and Planetary Science Letters*, *48*(2), 239–249. https://doi.org/10.1016/0012-821X(80)90187-9

Elsinger, R. J., & Moore, W. S. (1984). 226Ra and 228Ra in the mixing zones of the Pee Dee River-Winyah Bay, Yangtze river and Delaware Bay estuaries. *Estuarine, Coastal, and Shelf Science*, *18*(6), 601–613. https://doi.org/10.1016/0272-7714(84)90033-7

Gordeev, V. V. (2006). Fluvial sediment flux to the Arctic Ocean. *Geomorphology*, *80*(1–2), 94–104. https://doi.org/10.1016/j.geomorph.2005.09.008

Gordeev, V. V., Martin, J. M., Sidorov, I. S., & Sidorova, M. V. (1996). A reassessment of the Eurasian river input of water, sediment, major elements, and nutrients to the Arctic Ocean. *American Journal of Science*, *296*(6), 664–691. https://doi.org/10.2475/ajs.296.6.664

Grosfeld, K., Treffeisen, R., Asseng, J., Bartsch, A., Bräuer, B., Fritzsch, B., et al. (2015). Online sea-ice knowledge and data platform. *Polarforschung*, *85*(2), 143–155. https://doi.org/10.2312/polfor.2016.011

Guay, C. K., & Falkner, K. K. (1998). A survey of dissolved barium in the estuaries of major Arctic rivers and adjacent seas. *Continental Shelf Research*, *18*(8), 859–882. https://doi.org/10.1016/S0278-4343(98)00023-5

Günther, F., Overduin, P. P., Sandakov, A. V., Grosse, G., & Grigoriev, M. N. (2013). Short- and long-term thermo-erosion of ice-rich permafrost coasts in the Laptev Sea region. *Biogeosciences*, *10*(6), 4297–4318. https://doi.org/10.5194/bg-10-4297-2013

Haine, T. W. N., Curry, B., Gerdes, R., Hansen, E., Karcher, M., Lee, C., et al. (2015). Arctic freshwater export: Status, mechanisms, and prospects. *Global and Planetary Change*, *125*, 13–35. https://doi.org/10.1016/j.gloplacha.2014.11.013

Holmes, R. M., McClelland, J. W., Peterson, B. J., Shiklomanov, I. A., Shiklomanov, A. I., Zhulidov, A. V., et al. (2002). A circumpolar perspective on fluvial sediment flux to the Arctic Ocean. *Global Biogeochemical Cycles*, *16*(4), 1098–45-14. https://doi.org/10.1029/2001GB001849

Holmes, R. M., McClelland, J. W., Peterson, B. J., Tank, S. E., Bulygina, E., Eglinton, T. L., et al. (2012). Seasonal and annual fluxes of nutrients and organic matter from large rivers to the Arctic Ocean and surrounding seas. *Estuaries and Coasts*, *35*(2), 369–382. https://doi.org/10.1007/s12237-011-9386-6

Holmes, R. M., McClelland, J. W., Tank, S. E., Spencer, R. G. M., & Shiklomanov, A. I. (2021). *Arctic Great rivers observatory*. Water Quality Dataset & Absorbance Dataset. Version 2022/04/05. Retrieved from https://www.arcticgreatrivers.org/data

International Hydrographic Organization (IHO). (2001). Limits of Ocean and Seas, rep. S-23, draft (4th ed.).

IPCC. (2021). Climate change 2021: The physical science basis. In V.Masson-Delmotte, P. Zhai, A. Pirani, S. L. Connors, C. Péan, Y. Chen, L. Goldfarb, et al., (Eds)., *Contribution of working group I to the sixth assessment report of the intergovernmental panel on climate change*. Cambridge University Press. In Press. Retrieved from https://www.ipcc.ch/report/sixth-assessment-report-working-group-i/

Irrgang, A. M., Bendixen, M., Farquharson, L. M., Baranskaya, A. V., Erikson, L. H., Gibbs, A. E., et al. (2022). Drivers, dynamics, and impacts of changing Arctic coasts. *Nature Reviews Earth & Environment*, *3*(1), 39–54. https://doi.org/10.1038/s43017-021-00232-1

Jakobsson, M. (2002). Hypsometry and volume of the Arctic Ocean and its constituent seas. *Geochemistry, Geophysics, Geosystems*, *3*(5), 1–18. https://doi.org/10.1029/2001GC000302

Kadko, D., & Muench, R. (2005). Evaluation of shelf-basin interaction in the Western Arctic by use of short-lived radium isotopes: The importance of mesoscale processes. *Deep Sea Research Part II: Topical Studies in Oceanography*, *52*(24–26), 3227–3244. https://doi.org/10.1016/j.dsr2.2005.10.008

Key, R. M., Brewer, R. L., Stockwell, J. H., Guinasso, N. L., Jr., & Schink, D. R. (1979). Some improved techniques for measuring radon and radium in marine sediments and in seawater. *Marine Chemistry*, *7*(3), 251–264. https://doi.org/10.1016/0304-4203(79)90042-2

Key, R. M., Stallard, R. F., Moore, W. S., & Sarmiento, J. L. (1985). Distribution and flux of Ra-226 in the Amazon River estuary. *Journal of Geophysical Research*, *90*(C4), 6995–7004. https://doi.org/10.1029/jc090ic04p06995

Kipp, L. E., Charette, M. A., Moore, W. S., Henderson, P. B., & Rigor, I. G. (2018). Increased fluxes of shelf-derived materials to the central Arctic Ocean. *Science Advances*, *4*(1). eaao1302. https://doi.org/10.1126/sciadv.aao1302

Kipp, L. E., Henderson, P. B., Wang, Z. A., & Charette, M. A. (2020). Deltaic and estuarine controls on Mackenzie river solute fluxes to the Arctic Ocean. *Estuaries and Coasts*, *43*(8), 1992–2014. https://doi.org/10.1007/s12237-020-00739-8

Kipp, L. E., Kadko, D. C., Pickart, R. S., Henderson, P. B., Moore, W. S., & Charette, M. A. (2019). Shelf-basin interactions and water mass residence times in the Western Arctic Ocean: Insights provided by radium isotopes. *Journal of Geophysical Research: Oceans*, *124*(5), 3279–3297. https://doi.org/10.1029/2019JC014988

Kipp, L. E., Sanial, V., Henderson, P. B., van Beek, P., Reyss, J.-L., Hammond, D. E., et al. (2018b). Radium isotopes as tracers of hydrothermal inputs and neutrally buoyant plume dynamics in the deep ocean. *Marine Chemistry*, *201*, 51–65. https://doi.org/10.1016/j.marchem.2017.06.011

Klunder, M. B., Bauch, D., Laan, P., de Baar, H. J. W., van Heuven, S., & Ober, S. (2012). Dissolved iron in the Arctic shelf seas and surface waters of the central Arctic Ocean: Impact of Arctic river water and ice-melt. *Journal of Geophysical Research*, *117*(C1), C01027. https://doi.org/10.1029/2011JC007133

Krest, J. M., Moore, W. S., & Rama (1999). 226Ra and 228Ra in the mixing zones of the Mississippi and Atchafalaya Rivers: Indicators of groundwater input. *Marine Chemistry*, *64*(3), 129–152. https://doi.org/10.1016/S0304-4203(98)00070-X

Ku, T.-L., & Luo, S. (1994). New appraisal of Radium 226 as a large-scale oceanic mixing tracer. *Journal of Geophysical Research*, *99*(C5), 10255–10273. https://doi.org/10.1029/94JC00089

Ku, T.-L., & Luo, S. (2008). Ocean circulation/mixing studies with decay-series isotopes. In S. Krishnaswami & J. Kirk Cochran (Eds.) *Radioactivity in the Environment* (Vol. 13, pp. 307–344). Elsevier. https://doi.org/10.1016/S1569-4860(07)00009-5

Kuzyk, Z. Z. A., Macdonald, R. W., Johannessen, S. C., Gobeil, C., & Stern, G. A. (2009). Towards a sediment and organic carbon budget for Hudson Bay. *Marine Geology*, *264*(3–4), 190–208. https://doi.org/10.1016/j.margeo.2009.05.006

Kwon, E. Y., Kim, G., Primeau, F., Moore, W. S., Cho, H.-M., DeVries, T., et al. (2014). Global estimate of submarine groundwater discharge based on an observationally constrained radium isotope model. *Geophysical Research Letters*, *41*(23), 8438–8444. https://doi.org/10.1002/2014GL061574

Lammers, R. B., Shiklomanov, A. I., Vörösmarty, C. J., Fekete, B. M., & Peterson, B. J. (2001). Assessment of contemporary Arctic river runoff based on observational discharge records. *Journal of Geophysical Research*, *106*(D4), 3321–3334. https://doi.org/10.1029/2000JD900444

Lecher, A. L., Chien, C.-T., & Paytan, A. (2016). Submarine groundwater discharge as a source of nutrients to the North Pacific and Arctic coastal ocean. *Marine Chemistry*, *186*, 167–177. https://doi.org/10.1016/j.marchem.2016.09.008

Lecher, A. L., Kessler, J., Sparrow, K., Kodovska, F. G.-T., Dimova, N., Murray, J., et al. (2016). Methane transport through submarine groundwater discharge to the North Pacific and Arctic Ocean at two Alaskan sites. *Limnology and Oceanography*, *61*(S1), S344–S355. https://doi.org/10.1002/lno.10118

Le Gland, G., Mémery, L., Aumont, O., & Resplandy, L. (2017). Improving the inverse modeling of a trace isotope: How precisely can radium-228 fluxes toward the ocean and submarine groundwater discharge be estimated. *Biogeosciences*, *14*(13), 3171–3189. https://doi.org/10.5194/bg-14-3171-2017

Li, Y.-H., & Chan, L.-H. (1979). Desorption of Ba and 226Ra from River-borne sediments in the Hudson estuary. *Earth and Planetary Science Letters*, *43*(3), 343–350. https://doi.org/10.1016/0012-821X(79)90089-X

Li, Y.-H., Mathieu, G., Biscaye, P., & Simpson, H. J. (1977). The flux of 226Ra from estuarine and continental shelf sediments. *Earth and Planetary Science Letters*, *37*(2), 237–241. https://doi.org/10.1016/0012-821X(77)90168-6

Linhoff, B., Charette, M., & Wadham, J. (2020). Rapid mineral surface weathering beneath the Greenland Ice Sheet shown by radium and uranium isotopes. *Chemical Geology*, *547*(5), 119663. https://doi.org/10.1016/j.chemgeo.2020.119663

Luek, J. L., & Beck, A. J. (2014). Radium Budget of the York River estuary (VA, USA) dominated by submarine groundwater discharge with a seasonally variable groundwater end-member. *Marine Chemistry*, *165*, 55–65. https://doi.org/10.1016/j.marchem.2014.08.001

McClelland, J. W., Holmes, R. M., Dunton, K. H., & Macdonald, R. W. (2012). The Arctic Ocean estuary. *Estuaries and Coasts*, *35*(2), 353–368. https://doi.org/10.1007/s12237-010-9357-3

McClelland, J. W., Holmes, R. M., Peterson, B. J., Raymond, P. A., Striegl, R. G., Zhulidov, A. V., et al. (2016). Particulate organic carbon and nitrogen export from major Arctic rivers. *Global Biogeochemical Cycles*, *30*(5), 629–643. https://doi.org/10.1002/2015GB005351

Middag, R., de Baar, H. J. W., Laan, P., & Klunder, M. B. (2011). Fluvial and hydrothermal input of manganese into the Arctic Ocean. *Geochimica et Cosmochimica Acta*, *75*(9), 2393–2408. https://doi.org/10.1016/j.gca.2011.02.011

Moore, W., & Shaw, T. (2008). Fluxes and behavior of radium isotopes, barium, and uranium in seven Southeastern US rivers and estuaries. *Marine Chemistry*, *108*(3–4), 236–254. https://doi.org/10.1016/j.marchem.2007.03.004

Moore, W. D., & de Oliveira, J. (2008). Determination of residence time and mixing processes of the Ubatuba, Brazil, Inner shelf waters using natural Ra isotopes. *Estuarine, Coastal, and Shelf Science*, *76*(3), 512–521. https://doi.org/10.1016/j.ecss.2007.07.042

Moore, W. S. (2008). Fifteen years experience in measuring 224Ra and 223Ra by delayed-coincidence counting. *Marine Chemistry*, *109*(3–4), 188–197. https://doi.org/10.1016/j.marchem.2007.06.015

Moore, W. S., & Edmond, J. L. (1984). Radium and barium in the Amazon river system. *Journal of Geophysical Research*, *89*(C2), 2061–2065. https://doi.org/10.1029/JC089iC02p02061

Moore, W. S., & Krest, J. (2004). Distribution of 223Ra and 224Ra in the plumes of the Mississippi and Atchafalaya rivers and the Gulf of Mexico. *Marine Chemistry*, *86*(3–4), 105–119. https://doi.org/10.1016/j.marchem.2003.10.001

Moore, W. S., Sarmiento, J. L., & Key, R. M. (1986). Tracing the Amazon component of surface Atlantic water using 228Ra, salinity and silica. *Journal of Geophysical Research*, *91*(C2), 2574–2580. https://doi.org/10.1029/JC091iC02p02574

Moore, W. S., Sarmiento, J. L., & Key, R. M. (2008). Submarine groundwater discharge revealed by ^{228}Ra distribution in the upper Atlantic Ocean. *Nature Geoscience*, *1*(5), 309–311. https://doi.org/10.1038/ngeo183

Moore, W. S., & Shaw, T. J. (1998). Chemical signals from submarine fluid advection onto continental shelf. *Journal of Geophysical Research*, *103*(C10), 21543–21552. https://doi.org/10.1029/98JC02232

Moore, W. S., & Todd, J. F. (1993). Radium isotopes in the Orinoco estuary and eastern Caribbean Sea. *Journal of Geophysical Research*, *98*(C2), 2233–2244. https://doi.org/10.1029/92JC02760

Nielson, B. T., Cardenas, M. B., O'Connor, M. T., Rasmussen, M. T., King, T. V., & Kling, G. W. (2018). Groundwater flow and exchange across the land surface explain carbon export patterns in continuous permafrost watersheds. *Geophysical Research Letters*, *45*(15), 7596–7605. https://doi.org/10.1029/2018GL078140

Overeem, I., Hudson, B. D., Syvitski, J. P. M., Mikkelsen, A. B., Hasholt, B., van den Broeke, M. R., et al. (2017). Substantial export of suspended sediment to the global oceans from glacial erosion in Greenland. *Nature Geoscience*, *10*(11), 859–863. https://doi.org/10.1038/ngeo3046

Peterson, R. N., Burnett, W. C., Opsahl, S. P., Santos, I. R., Misra, S., & Froelich, P. N. (2013). Tracking suspended particle transport via radium isotopes (^{226}Ra and ^{228}Ra) through the Apalachicola-Chattahoochee-Flint River system. *Journal of Environmental Radioactivity*, *116*, 65–75. https://doi.org/10.1016/j.jenvrad.2012.09.001

Rainville, L., & Woodgate, R. A. (2009). Observations of internal wave generation in the seasonally ice-free Arctic. *Geophysical Research Letters*, *36*(23), L23604. https://doi.org/10.1029/2009GL041291

Rawlins, M. A., Steele, M., Holland, M. M., Adam, J. C., Cherry, J. E., Francis, J. A., et al. (2010). Analysis of the Arctic system for freshwater cycle intensification: Observations and expectations. *Journal of Climate*, *23*(21), 5715–5737. https://doi.org/10.1175/2010JCLI3421.1

Rudels, B., Korhonen, M., Schauer, U., Pisarev, S., Rabe, B., & Wisotzki, A. (2015). Circulation and transformation of Atlantic water in the Eurasian Basin and the contribution of the Fram Strait inflow branch to the Arctic Ocean heat budget. *Progress in Oceanography*, *132*, 128–152. https://doi.org/10.1016/j.pocean.2014.04.003

Rutgers van der Loeff, M., Key, R. M., Scholten, J., Bauch, D., & Michel, A. (1995). 228Ra as a tracer for shelf water in the Arctic Ocean. *Deep Sea Research Part II: Topical Studies in Oceanography*, *42*(6), 1533–1553. https://doi.org/10.1016/0967-0645(95)00053-4

Rutgers van der Loeff, M., Kipp, L. E., Charette, M. A., Moore, W. S., Black, E., Ingrid, S., et al. (2018). Radium isotopes across the Arctic Ocean show time scales of water mass ventilation and increasing shelf inputs. *Journal of Geophysical Research: Oceans*, *123*(7), 4853–4873. https://doi.org/10.1029/2018JC013888

Rutgers van der Loeff, M., Kühne, S., Wahsner, M., Höltzer, H., Frank, M., Ekwurzel, B., et al. (2003). 228Ra and 226Ra in the Kara and Laptev seas. *Continental Shelf Research*, *23*(1), 113–124. https://doi.org/10.1016/S0278-4343(02)00169-3

Sérodes, J.-B., & Roy, J.-C. (1983). Distribution of some radionuclides in the St. Lawrence estuary, Quebec, Canada. *Oceanologica Acta*, *6*(2), 185–192.

Serreze, M. C., Barret, A. P., Slater, A. G., Woodgate, R. A., Aagaard, K., Lammers, R. B., et al. (2006). The large-scale freshwater cycle of the Arctic. *Journal of Geophysical Research*, *111*(C11), C11010. https://doi.org/10.1029/2005JC003424

Suzuki, T., Yamazaki, D., Tsujino, H., Komuro, Y., Nakano, H., & Urakawa, S. (2018). A dataset of continental river discharge based on JRA-55 for use in a global ocean circulation model. *Journal of Oceanography*, *74*(4), 421–429. https://doi.org/10.1007/s10872-017-0458-5

Tomasky-Holmes, G., Valiela, I., & Charette, M. A. (2013). Determination of water mass ages using radium isotopes as tracers: Implications for phytoplankton dynamics in estuaries. *Marine Chemistry*, *156*, 18–26. https://doi.org/10.1016/j.marchem.2013.02.002

Vieira, L. H., Achterberg, E. P., Scholten, J., Beck, A. J., Liebetrau, V., Mills, M. M., & Arrigo, K. R. (2019). Benthic fluxes of trace metals in the Chukchi Sea and their transport into the Arctic Ocean. *Marine Chemistry*, *208*, 43–55. https://doi.org/10.1016/j.marchem.2018.11.001

Wang, P., Huang, Q., Pozdniakov, S. P., Liu, S., Ma, N., Wang, T., et al. (2021). Potential role of permafrost thaw on increasing Siberian river discharge. *Environmental Research Letters*, *16*(3), 034046. https://doi.org/10.1088/1748-9326/abe326

Webster, I. T., Hancock, G. J., & Murray, A. S. (1995). Modelling the effect of salinity on radium desorption from sediments. *Geochimica et Cosmochimica Acta*, *59*(12), 2469–2476. https://doi.org/10.1016/0016-7037(95)00141-7

Wheeler, P. A., Watkins, J. M., & Hansing, R. L. (1997). Nutrients, organic carbon and organic nitrogen in the upper water column of the Arctic Ocean: Implications for the sources of dissolved organic carbon. *Deep Sea Research Part II: Topical Studies in Oceanography*, *44*(8), 1571–1592. https://doi.org/10.1016/s0967-0645(97)00051-9

Williams, W. J., & Carmack, E. C. (2015). The 'interior' shelves of the Arctic Ocean: Physical oceanographic setting, climatology and effects of sea-ice retreat on cross-shelf exchange. *Progress in Oceanography*, *139*, 24–41. https://doi.org/10.1016/j.pocean.2015.07.008

Woodgate, R. A., Weingartner, T. J., & Lindsay, R. (2012). Observed increases in Bering Strait oceanic fluxes from the Pacific to the Arctic from 2001 to 2011 and their impacts on the Arctic Ocean water column. *Geophysical Research Letters*, *39*(24), 2012GL054092. https://doi.org/10.1029/2012GL054092

Xu, B., Li, S., Burnett, W. C., Zhao, S., Santos, I., Lian, E., et al. (2022). Radium-226 in the global ocean as a tracer of the thermohaline circulation: Synthesizing half a century of observations. *Earth-Science Reviews*, *226*, 103956. https://doi.org/10.1016/j.earscirev.2022.103956

References From the Supporting Information

Abitu, E. K., Oliveira, J. M., Malta, M., Santos, M., Mulaji, C. K., Mpiana, P. T., & Carvalho, F. P. (2021). Assessment of natural radioactivity in rivers sediment and soil from the copper belt Artisanal mining region, Democratic Republic of Congo. *Journal of Geoscience and Environment Protection*, *9*(7). https://doi.org/10.4236/gep.2021.97001

Allison, M. A., Demas, C. R., Ebersole, B. A., Kleiss, B. A., Little, C. D., Meselhe, E. A., et al. (2012). A water and sediment budget for the lower Mississippi-Atchafalaya river in flood years 2008-2010: Implications for sediment discharge to the oceans and coastal restoration in Louisiana. *Journal of Hydrology*, *432–433*, 84–97. https://doi.org/10.1016/j.jhydrol.2012.02.020

Benke, A. C., & Cushing, C. E. (2005). *Rivers of North America*. Academic Press. https://doi.org/10.1016/B978-012088253-3/50003-1

Beszczynska-Möller, A., Fahrbach, E., Schauer, U., & Hansen, E. (2012). Variability in Atlantic water temperature and transport at the entrance to the Arctic Ocean, 1997 - 2010. *ICES Journal of Marine Science*, *69*(5), 852–863. https://doi.org/10.1093/icesjms/fss056

Brabets, T. P., Nelson, G. L., Dorava, J. M., & Milner, A. M. (1999). Water-quality assessment of the Cook Inlet Basin, Alaska - Environmental setting. In E. F. Snyder, L.-L. Harris, & S. L. Benson (Eds.), *Water-resources investigations report 99-4025*. U.S. Geological Survey.

Breier, J. A., Breier, C. F., & Edmonds, H. N. (2005). Detecting submarine groundwater discharge with synoptic surveys of sediment resistivity, radium, and salinity. *Geophysical Research Letters*, *32*(23), L23612. https://doi.org/10.1029/2005GL024639

Bridgestock, L., Nathan, J., Paver, R., Hsieh, Y.-T., Porcelli, D., Tanzil, J., et al. (2021). Estuarine processes modify the isotope composition of dissolved riverine barium fluxes to the ocean. *Chemical Geology*, *579*, 120340. https://doi.org/10.1016/j.chemgeo.2021.120340

Carson, M. A., Jasper, J. N., & Conly, F. M. (1998). Magnitude and sources of sediment input to the Mackenzie delta, Northwest Territories, 1974-94. *Arctic*, *51*(2), 116–124. https://doi.org/10.14430/arctic1053

Chalov, S., Liu, S., Chalov, R. S., Chalova, E. R., Chernov, A. V., Promakhova, E. V., et al. (2018). Environmental and human impacts on sediment transport of the largest Asian rivers of Russia and China. *Environmental Earth Sciences*, *77*(7), 274. https://doi.org/10.1007/s12665-018-7448-9

Charette, M. A. (2007). Hydrologic forcing of submarine groundwater discharge: Insight from a seasonal study of radium isotopes in a groundwater-dominated salt marsh estuary. *Limnology and Oceanography*, *52*(1), 230–239. https://doi.org/10.4319/lo.2007.52.1.0230

Charette, M. A., & Buesseler, K. O. (2004). Submarine groundwater discharge of nutrients and copper to an urban subestuary of Chesapeake Bay (Elizabeth river). *Limnology and Oceanography*, *49*(2), 376–385. https://doi.org/10.4319/lo.2004.49.2.0376

Charette, M. A., Henderson, P. B., Breier, C. F., & Liu, Q. (2013). Submarine groundwater discharge in a river-dominated Florida estuary. *Marine Chemistry*, *156*, 3–17. https://doi.org/10.1016/j.marchem.2013.04.001

Chen, Z., Shen, H., & Zhanghua, W. (2001). Yangtze river of China: Historical analysis of discharge variability and sediment flux. *Geomorphology*, *41*(2–3), 77–91. https://doi.org/10.1016/s0169-555x(01)00106-4

Crotwell, A. M., & Moore, W. S. (2003). Nutrient and radium fluxes from submarine groundwater discharge to Port Royal Sound, South Carolina. *Aquatic Geochemistry*, *9*(3), 191–208. https://doi.org/10.1023/B:AQUA.0000022954.89019.c9

Dai, G., Wang, G., Li, Q., Tan, E., & Dai, M. (2021). Submarine groundwater discharge on the Western shelf of the Northern South China Sea influenced by the pearl river plume and upwelling. *Journal of Geophysical Research: Oceans*, *126*(4), e2020JC016859. https://doi.org/10.1029/2020JC016859

Dias, T. H., de Oliveira, J., Sanders, C. J., Carvalho, F., Sanders, L. M., Machado, E. C., & Sá, F. (2016). Radium isotope (223Ra, 224Ra, 226Ra and 228Ra) distribution near Brazil's largest port, Paranaguá Bay. *Brazilian Marine Pollution Bulletin*, *111*(1–2), 443–448. https://doi.org/10.1016/j.marpolbul.2016.07.004

Du, J., Moore, W. S., Zhang, G., Su, N., & Zhang, J. (2013). Nutrient inputs to a Lagoon through submarine groundwater discharge: The case of Laoye Lagoon, Hainan, China. *Journal of Marine Systems*, *111–112*, 253–262. https://doi.org/10.1016/j.jmarsys.2012.11.007

Dulaiova, H., Burnett, W. C., Chanton, J. P., Moore, W. S., Bokuniewicz, H. J., Charette, M. A., & Sholkovitz, E. (2006). Assessment of groundwater discharges into West Neck Bay, New York, via natural tracers. *Continental Shelf Research*, *26*(16), 1971–1983. https://doi.org/10.1016/j.csr.2006.07.011

Forbes, D. L. (1981). *Babbage River delta and lagoon: Hydrology and sedimentology of an Arctic estuarine system*. PhD Thesis, University of British Columbia.

Garcia-Solsona, E., Garcia-Orellana, J., Masqué, P., & Dulaiova, H. (2008). Uncertainties associated with 223Ra and 224Ra measurements in water via a delayed coincidence counter (RaDeCC). *Marine Chemistry*, *109*(3–4), 198–219. https://doi.org/10.1016/j.marchem.2007.11.006

Garcia-Solsona, E., Garcia-Orellana, J., Masqué, P., Rodellas, V., Mejías, M., Ballesteros, B., & Domínguez, J. A. (2010). Groundwater and nutrient discharge through Karstic coastal springs (Castelló, Spain). *Biogeosciences*, *7*(9), 2625–2638. https://doi.org/10.5194/bg-7-2625-2010

Garzanti, E., Andó, S., France-Lanord, C., Censi, P., Vignola, P., Galy, V., & Lupker, M. (2011). Mineralogical and chemical variability of fluvial sediments 2. Suspended-load silt (Ganga-Brahmaputra, Bangladesh). *Earth and Planetary Science Letters*, *302*(1–2), 107–120. https://doi.org/10.1016/j.epsl.2010.11.043

George, C., Moore, W. S., White, S. M., Smoak, E., Joye, S. B., Leier, A., & Wilson, A. M. (2020). A new mechanism for submarine groundwater discharge from continental shelves. *Water Resources Research*, *56*(11), e2019WR026866. https://doi.org/10.1029/2019WR026866

Godoy, J. M., de Carvalho, Z. L., da Costa Fernandes, F., Danelon, O. M., Godoy, M. L. D. P., Ferreira, A. C. M., & Roldão, L. A. (2006). ^{228}Ra and ^{226}Ra in coastal seawater samples from the Ubatuba region - Brazilian Southwestern Coastal Region. *Journal of the Brazilian Chemical Society*, *17*(4), 730–736. https://doi.org/10.1590/S0103-50532006000400014

Gonneea, M. E., Mulligan, A. E., & Charette, M. A. (2013). Seasonal cycles in radium and barium within a subterranean estuary: Implications for groundwater derived chemical fluxes to surface waters. *Geochimica et Cosmochimica Acta*, *119*, 164–177. https://doi.org/10.1016/j.gca.2013.05.034

Gordeev, V. V., Rachold, V., & Vlasova, I. E. (2004). Geochemical behaviour of major and trace elements in suspended particulate material of the Irtysh river, the main tributary of the Ob river, Siberia. *Applied Geochemistry*, *19*(4), 593–610. https://doi.org/10.1016/j.apgeochem.2003.08.004

Gu, H., Moore, W. S., Zhang, L., Du, J., & Zhang, J. (2012). Using radium isotopes to estimate the residence time and the contribution of submarine groundwater discharge (SGD) in the Changjiang effluent plume, East China Sea. *Continental Shelf Research*, *35*, 95–107. https://doi.org/10.1016/j.csr.2012.01.002

Isupova, M. V., & Mikhailov, V. N. (2018). Long-term variations of water runoff and suspended sediment yield in the Parana and Uruguay rivers. *Water Research*, *45*(6), 846–860. https://doi.org/10.1134/s0097807818060088

Jones, S. H., Madison, R. J., & Zenone, C. (1978). Water resources of the Kodiak-Shelikof subregion, South-Central Alaska. In *Hydrologic investigations Atlas HA-612*. U.S. Geological Survey.

Knott, J. M., Lipscomb, S. W., & Lewis, T. W. (1986). *Sediment transport characteristics of selected streams in the Susitna River Basin, Alaska, October 1983 to September 1984*. In U.S. Geological Survey, Open-File Report 86 - 424W. U.S. Geological Survey.

Krest, J. M., Moore, W. S., Gardner, L. R., & Morris, J. T. (2000). Marsh nutrient export supplied by groundwater discharge: Evidence from radium measurements. *Global Biogeochemistry Cycles*, *14*(1), 167–176. https://doi.org/10.1029/1999GB001197

Kummu, M., & Varis, O. (2007). Sediment-related impacts due to upstream reservoir trapping, the Lower Mekong River. *Geomorphology*, *85*(3–4), 275–293. https://doi.org/10.1016/j.geomorph.2006.03.024

Lai, C., Chen, X., Wang, Z., Wu, X., Zhao, S., Wu, X., & Bai, W. (2016). Spatio-temporal variation in rainfall erosivity during 1960 - 2012 in the Pearl River Basin, China. *CATENA*, *137*, 382–391. https://doi.org/10.1016/j.catena.2015.10.008

Lamontagne, S., Taylor, A. R., Herpich, D., & Hancock, G. J. (2015). Submarine groundwater discharge from the South Australian Limestone Coast region estimated using radium and salinity. *Journal of Environmental Radioactivity*, *140*, 30–41. https://doi.org/10.1016/j.jenvrad.2014.10.013

Laraque, A., Castellanos, B., Steiger, J., Lòpez, J. L., Pandi, A., Rodriguez, M., et al. (2013). A comparison of the suspended and dissolved matter dynamics of two large inter-tropical rivers draining into the Atlantic Ocean: The Congo and the Orinoco. *Hydrological Processes*, *27*(15), 2153–2170. https://doi.org/10.1002/hyp.9776

Legeleux, F., & Reyss, J.-L. (1996). ^{228}Ra/^{226}Ra activity ratio in oceanic settling particles: Implications regarding the use of barium as a proxy for paleoproductivity reconstruction. *Deep Sea Research I*, *43*(11–12), 1857–1863. https://doi.org/10.1016/s0967-0637(96)00086-6

Li, Q., Qiao, S., Shi, X., Hu, L., Bai, Y., Zhu, A., & Cui, J. (2020). Sediment provenance of the East Siberian Arctic shelf: Evidence from clay minerals and chemical elements. EGU General Assembly, 2020. Online, EGU2020-8181. https://doi.org/10.5194/egusphere-egu2020-8181

Lima, J. E. F. W., Santos, P. M. C., Carvalho, N. O., & Silva, E. M. (2003). *Diagnóstico do fluxo de sedimentos em suspensão na Bacia Araguaia-Tocantins*. Embrapa Cerrados/ANEEL/ANA.

Liu, Y., Jiao, J. J., Mao, R., Luo, X., Liang, W., & Robinson, C. (2019). Spatial characteristics reveal the reactive transport of radium isotopes (224Ra, 223Ra, and 228Ra) in an Intertidal aquifer. *Water Resources Research*, *55*(12), 10282–10302. https://doi.org/10.1029/2019WR024849

Luo, X., Jiao, J. J., Liu, Y., Zhang, X., Liang, W., & Tang, D. (2018). Evaluation of water residence time, submarine groundwater discharge, and maximum new production supported by groundwater borne nutrients in a coastal upwelling shelf system. *Journal of Geophysical Research: Oceans*, *123*(1), 631–655. https://doi.org/10.1002/2017JC013398

Martinez, J. M., Guyot, J. L., Filizola, N., & Sondag, F. (2009). Increase in suspended sediment discharge of the Amazon River assessed by monitoring network and satellite data. *Catena*, *79*(3), 257–264. https://doi.org/10.1016/j.catena.2009.05.011

Meybeck, M., & Ragu, A. (1997). *River discharges to the oceans: An assessment of suspended solids, major ions and nutrients* (Vol. 245). UNEP.

Meybeck, M., & Ragu, A. (2012). *GEMS-GLORI world river discharge database*. Laboratoire de Géologie Appliquée, Université Pierre et Marie Curie. https://doi.org/10.1594/PANGAEA.804574

Milliman, J., & Farnsworth, K. (2011). *River discharge to the Coastal Ocean: A global synthesis*. Cambridge University Press. https://doi.org/10.1017/CBO9780511781247

Milliman, J., & Syvitski, J. (1992). Geomorphic/tectonic control of sediment discharge to the ocean: The importance of small mountainous rivers. *Journal of Geology*, *100*(5), 525–544. https://doi.org/10.1086/629606

Moore, W. S. (2003). Sources and fluxes of submarine groundwater discharge delineated by radium isotopes. *Biogeochemistry*, *66*(1/2), 75–93. https://doi.org/10.1023/b:biog.0000006065.77764.a0

Moore, W. S., Blanton, J. O., & Joye, S. (2006). Estimates of flushing times, submarine groundwater discharge, and nutrient fluxes to Okatee river, South Carolina. *Journal of Geophysical Research*, *111*(C9), C09006. https://doi.org/10.1029/2005JC003041

Moore, W. S., Krest, J., Taylor, G., Roggenstein, E., Joye, S., & Lee, R. (2002). Thermal evidence of water exchange through a coastal aquifer: Implications for nutrient fluxes. *Geophysical Research Letters*, *29*(14), 49-1–49-4. https://doi.org/10.1029/2002GL014923

Moore, W. S., & Wilson, A. M. (2005). Advective flow through the upper continental shelf driven by storms, buoyancy, and submarine groundwater discharge. *Earth and Planetary Sciences Letters*, *235*(3–4), 564–576. https://doi.org/10.1016/j.epsl.2005.04.043

Moragoda, N., & Cohen, S. (2020). Climate-induced trends in global riverine water discharge and suspended sediment dynamics in the 21st century. *Global and Planetary Change*, *191*, 103199. https://doi.org/10.1016/j.gloplacha.2020.103199

Morehead, M. D., Syvitski, J. P., Hutton, E. W. H., & Peckham, S. D. (2003). Modeling the temporal variability in the flux of sediment from ungauged river basins. *Global and Planetary Change*, *39*(1–2), 95–110. https://doi.org/10.1016/S0921-8181(03)00019-5

Mulder, T., Savoye, B., Piper, D. J. W., & Syvitski, J. P. M. (1998). The Var submarine sedimentary system: Understanding Holocene sediment delivery processes and their importance to the geological record. *Geological Society, London, Special Publications*, *129*(1), 145–166. https://doi.org/10.1144/GSL.SP.1998.129.01.10

Ollivier, P., Claude, C., Radakovitch, O., & Hamelin, B. (2008). TIMS measurements of 226Ra and 228Ra in the Gulf of Lion, an attempt to quantify submarine groundwater discharge. *Marine Chemistry*, *109*(3–4), 337–354. https://doi.org/10.1016/j.marchem.2007.08.006

Overeem, I., & Syvitski, J. (2008). *Changing sediment supply in Arctic rivers*. Paper presented at Sediment Dynamics in Changing Environments. National Institute of Water & Atmospheric Research (NIWA).

Pontér, C., Ingri, J., & Boström, K. (1992). Geochemistry of manganese in the Kalix River, northern Sweden. *Geochimica et Cosmochimica Acta*, *56*(4), 1485–1494. https://doi.org/10.1016/0016-7037(92)90218-8

Porcelli, D., Wasserburg, G. J., & Baskaran, M. (2001). Transport of U- and Th-series nuclides in a Baltic Shield watershed and the Baltic Sea. *Geochimica et Cosmochimica Acta*, *65*(15), 2439–2459. https://doi.org/10.1016/S0016-7037(01)00610-X

Potot, C. (2011). Etude hydrochimique du système aquifère de la basse vallée du Var Apport des éléments traces et des isotopes (Sr, Pb, δ18O, 226, 228Ra). Autre. Université Nice Sophia Antipolis, 2011.

Purkl, S., & Eisenhauer, A. (2004). Determination of radium isotopes and Rn-222 in a groundwater affected coastal area of the Baltic Sea and the underlying sub-sea floor aquifer. *Marine Chemistry*, *87*(3–4), 137–149. https://doi.org/10.1016/j.marchem.2004.02.005

Rama, & Moore, W. S. (1996). Using the radium quartet for evaluating groundwater input and water exchange in salt marshes. *Geochimica et Cosmochimica Acta*, *60*(23), 4645–4652. https://doi.org/10.1016/s0016-7037(96)00289-x

Robinson, R. A. J., Bird, M. I., Oo, N. W., Hoey, T. B., Aye, M. M., Higgitt, D. L., et al. (2007). The Irrawaddy river sediment flux to the Indian Ocean: The original nineteenth-centry data revisited. *Journal of Geology*, *115*(6), 629–640. https://doi.org/10.1086/521607

Rondeau, B., Cossa, D., Gagnon, P., & Bilodeau, L. (2000). Budget and sources of suspended sediment transported in the St. Lawrence River. *Canadan Hydrological Processes*, *14*(1), 21–36. https://doi.org/10.1002/(sici)1099-1085(200001)14:1<21::aid-hyp907>3.0.co;2-7

Sanial, V., Moore, W. S., & Shiller, A. M. (2021). Does a bottom-up mechanism promote hypoxia in the Mississippi Bight? *Marine Chemistry*, *235*, 104007. https://doi.org/10.1016/j.marchem.2021.104007

Sarin, M. M., Krishnaswami, S., Somayajulu, B. L. K., & Moore, W. S. (1990). Chemistry of uranium, thorium, and radium isotopes in the Ganga-Brahmaputra river system: Weathering processes and fluxes to the Bay of Bengal. *Geochimica et Cosmochimica Acta*, *54*(5), 1387–1396. https://doi.org/10.1016/0016-7037(90)90163-F

Smith, J. N., Moran, S. B., & Macdonald, R. W. (2003). Shelf-basin interactions in the Arctic Ocean based on ^{210}Pb and Ra isotope tracer distributions. *Deep Sea Research Part 1: Oceanographic Research Papers*, *50*(3), 397–416. https://doi.org/10.1016/S0967-0637(02)00166-8

Solin, G. L. (1996). *Overview of surface-water resources at the U.S. Coast Guard Support Center Kodiak, Alaska, 1987 - 1989*. In U.S. Geological Survey, Open-File Report 96-463. U.S. Geological Survey.

Su, N., Du, J., Duan, Z., Deng, B., & Zhang, J. (2015). Radium isotopes and their implications in the Changjiang River system. *Estuarine, Coastal and Shelf Science*, *156*, 155–164. https://doi.org/10.1016/j.ecss.2014.12.017

Swarzenski, P. W., Orem, W. H., McPherson, B. F., Baskam, M., & Wan, Y. (2006). Biochemical transport in the Loxahatchee River estuary, Florida: The role of submarine groundwater discharge. *Marine Chemistry*, *101*(3–4), 248–265. https://doi.org/10.1016/j.marchem.2006.03.007

Swarzenski, P. W., Reich, C. D., Kroeger, K. D., & Baskaran, M. (2007). Ra and Rn isotopes as natural tracers of submarine groundwater discharge in Tampa Bay, Florida. *Marine Chemistry*, *104*(1–2), 64–84. https://doi.org/10.1016/j.marchem.2006.08.001

Syvitski, J. P., Morehead, M. D., Bahr, D. B., & Mulder, T. (2000). Estimating fluvial sediment transport: The rating parameters. *Water Resources Research*, *36*(9), 2747–2760. https://doi.org/10.1029/2000wr900133

Syvitski, J. P. M. (2002). Sediment discharge variability in Arctic rivers: Implications for a warmer future. *Polar Research*, *21*(2), 323–330. https://doi.org/10.3402/polar.v21i2.6494

Tan, E., Wang, G., Moore, W. S., Li, Q., & Dai, M. (2018). Shelf-scale submarine groundwater discharge in the Northern South China Sea and East China Sea and its Geochemical impacts. *Journal of Geophysical Research: Oceans*, *123*(4), 2997–3013. https://doi.org/10.1029/2017JC013405

U.S. Geological Survey. (2016). National water information system data retrieved on July 17, 2020 from USGS water data for the Nation. Retrieved from https://waterdata.usgs.gov/nwis/uv?site_no=15284000

van Vliet, M. T. H., Wilberg, D., Leduc, S., & Riahi, K. (2013). Power-generation system vulnerability and adaptation to changes in climate and water resources. *Nature Climate Change Letters*, *6*(4), 375–381. https://doi.org/10.1038/nclimate2903

Viscosi-Shirley, C., Mammone, K., Pisias, N., & Dymond, J. (2003). Clay mineralogy and multi-element chemistry of surface sediments on the Siberian-Arctic shelf: Implications for sediment provenance and grain size sorting. *Continental Shelf Research*, *23*(11–13), 1175–1200. https://doi.org/10.1016/S0278-4343(03)00091-8

Walling, D. E. (2008). The changing sediment load of the Mekong River. *AMBIO*, *37*(3), 150–157. https://doi.org/10.1579/0044-7447(2008)37[150:tcslot]2.0.co;2

Wang, X., Li, H., Jiao, J. J., Barry, D. A., Li, L., Luo, L., et al. (2015). Submarine fresh groundwater discharge into Laizhou Bay comparable to the Yellow River flux. *Scientific Reports*, *5*(1), 8813. https://doi.org/10.1038/srep08814

Water Survey of Canada. (2020). Back, Ellice, Hornaday, Firth, Omoloy, and Babbage River records. Retrieved on July 17, 2020 from Environment and Climate Change Canada Historical Hydrometric Data web site Retrieved from https://wateroffice.ec.gc.ca/mainmenu/historical_data_index_e.html

Windham, H. L., Niencheski, L. F., Moore, W. S., & Jahnke, R. (2006). Submarine groundwater discharge: A large, previously unrecognized source of dissolved iron to the South Atlantic Ocean. *Marine Chemistry*, *102*(3–4), 252–266. https://doi.org/10.1016/j.marchem.2006.06.016

Yang, H.-S., Hwang, D.-W., & Kim, G. (2002). Factors controlling excess radium in the Nakdong River estuary, Korea: Submarine groundwater discharge versus desorption from riverine particles. *Marine Chemistry*, *78*, 1–8. https://doi.org/10.1016/S0304-4203(02)00004-X

Young, M. B., Gonneea, M. E., Fong, D. A., Moore, W. S., Herrera-Silveira, J., & Paytan, A. (2008). Characterizing sources of groundwater to a tropical coastal lagoon in a karstic area using radium isotopes and water chemistry. *Marine Chemistry*, *109*(3–4), 377–394. https://doi.org/10.1016/j.marchem.2007.07.010

Yunker, M. B., Backus, S. M., Pannatier, E. G., Jeffries, D. S., & Macdonald, R. W. (2002). Sources and significance of Alkane and PAH Hydrocarbons in Canadian Arctic Rivers. *Estuarine, Coastal, and Shelf Science*, *55*, 1–31. https://doi.org/10.1006/ecss.2001.0880